

Snow interception modelling: Isolated observations have led to many land surface models lacking appropriate temperature sensitivities

Jessica D. Lundquist¹  | Susan Dickerson-Lange²  | Ethan Gutmann³  | Tobias Jonas⁴  | Cassie Lumbrazo¹  | Dylan Reynolds^{1,4} 

¹Civil and Environmental Engineering, University of Washington, Seattle, Washington, USA

²Natural Systems Design, Seattle, Washington, USA

³National Center for Atmospheric Research, Boulder, Colorado, USA

⁴WSL Institute for Snow and Avalanche Research SLF, Davos Dorf, Switzerland

Correspondence

Jessica D. Lundquist, Civil and Environmental Engineering, University of Washington, Box 352700, Seattle, WA 98195, USA.
Email: jdlund@uw.edu

Funding information

NASA, Grant/Award Number: 80NSSC18K1405; National Science Foundation, Grant/Award Number: CBET-1703663

Abstract

When formulating a hydrologic model, scientists rely on parameterizations of multiple processes based on field data, but literature review suggests that more frequently people select parameterizations that were included in pre-existing models rather than re-evaluating the underlying field experiments. Problems arise when limited field data exist, when “trusted” approaches do not get reevaluated, and when sensitivities fundamentally change in different environments. The physics and dynamics of snow interception by conifers is just such a case, and it is critical to simulation of the water budget and surface albedo. The most commonly used interception parameterization is based on data from four trees from one site, but results from this field study are not directly transferable to locations with relatively warmer winters, where the dominant processes differ dramatically. Here, we combine a literature review with model experiments to demonstrate needed improvements. Our results show that the choice of model form and parameters can vary the fraction of snow lost through interception by as much as 30%. In most simulations, the warming of mean winter temperatures from -7 to 0°C reduces the modelled fraction of snow under the canopy compared to the open, but the magnitude of simulated decrease varies from about 10% to 40%. The range of results is even larger when considering models that neglect the melting of in-canopy snow in higher-humidity environments where canopy sublimation plays less of a role. Thus, we recommend that all models represent canopy snowmelt and include representation of increased loading due to increased adhesion and cohesion when temperatures rise from -3 to 0°C . In addition to model improvements, field experiments across climates and forest types are needed to investigate how to best model the combination of dynamically changing forest cover and snow cover to better understand and predict changes to albedo and water supplies.

KEYWORDS

albedo, forest, history, hydrology, interception, modelling, snow, vegetation

1 | INTRODUCTION

Both forest cover and snow processes are changing globally at unprecedented rates (Adams et al., 2009; Allen, 2009; Bormann

et al., 2018; Halofsky et al., 2020). These changes, their interactions, and their impacts are critical components of any model of the terrestrial water balance and energy balance. Substantial research has demonstrated that modelling forest–snow interactions is complicated

(Dickerson-Lange et al., 2017; Helbig et al., 2020; Rutter et al., 2009). However, global land surface model representations of canopy snow interception are currently based on observations from only two studies (Hedstrom & Pomeroy, 1998; Storck, 2000). Employing a larger literature review and an interception model, we propose how to improve process representation of accumulation, ablation, and unloading of snow in the forest canopy. These improvements are critical for models that span multiple climates (e.g., global, mountain, continental, maritime, and/or climate change applications), as many current parameterizations are not transferable in space or time.

Snow accumulation under forests compared to the open varies from 40% to nearly identical amounts, and these differences are the dominant drivers of net changes in snow accumulation and duration (Dickerson-Lange et al., 2017; Lundquist et al., 2013), which leads to differences in total runoff, particularly in summer streamflow (Cristea et al., 2014; Sun et al., 2018). Interception dynamics vary widely with forest structure and regional climate, as well as between individual storms (Carlyle-Moses & Gash, 2011; Lundquist et al., 2013; Moeser et al., 2015). However, given historic difficulty in measuring interception (Friesen et al., 2015), current measurements and understanding are limited to a few locations representing a minority of forest structures and climatic settings.

Due to a lack of better information, parameterizations that have been validated in only one specific setting are being used in global models, while parameterizations from another setting can differ in even the sign of their response to temperature (Andreadis et al., 2009; Clark

et al., 2015; Hedstrom & Pomeroy, 1998). Hedstrom and Pomeroy (1998) formulated maximum snow interception per unit vegetation area decreasing with temperature, due to increased snow rebound and decreased tree-branch stiffness, while Andreadis et al. (2009) described it increasing rapidly as temperatures warm above -3°C , due to increasing cohesiveness of snow at warmer temperatures (Figure 1(b)). While these two parameterizations match at low temperatures, a well-calibrated model subjected to warmer temperatures (e.g., for a climate sensitivity experiment) would show a different hydrologic response: interception will vary by a factor of four depending on the model chosen, with subsequent effects on snowpack and soil moisture. These two formulations are based on (Figure 1(d)) branches clipped to a pole in the Rocky Mountains (Schmidt & Gluns, 1991) or (Figure 1(e)) two Douglas Firs on weighing lysimeters in the Oregon Cascades (Storck, 2000) and provide the basis for the majority of our models.

Changes in land surface albedo are another important, yet poorly understood, feedback in global climate variability. Variability in land surface albedo between CMIP5 climate models can explain 40%–50% of the spread in modelled warming over the northern hemisphere (Qu & Hall, 2014; Thackeray & Fletcher, 2016), and intercepted snow in the canopy affects albedo by $\sim 24\%$ (Webster & Jonas, 2018). Model differences in how intercepted snow is removed from the canopy play an important role in the energy balance (Thackeray et al., 2014) but vary widely and may be a function of air temperature and wind speed (Roesch et al., 2001) or a constant rate, leading to exponential decay of canopy snow (Hedstrom & Pomeroy, 1998).

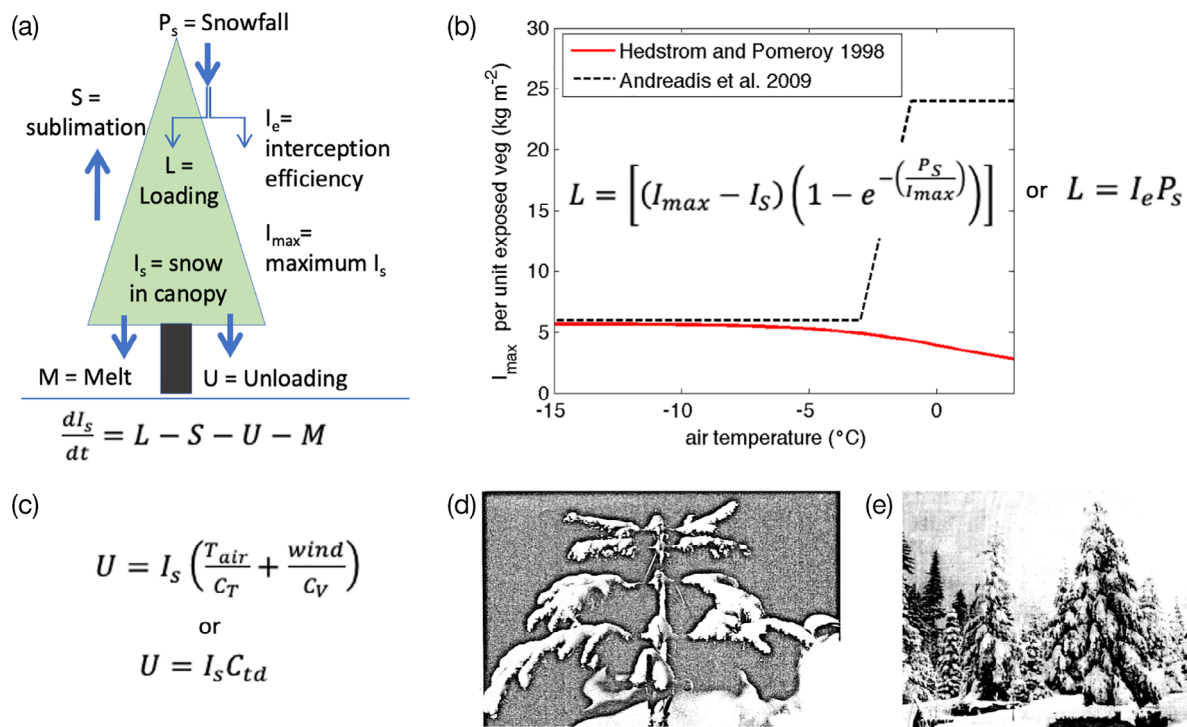


FIGURE 1 (a) Illustration of canopy processes and parameters in land surface models: Trees intercept snow with a fractional efficiency (I_e) up to a maximum value (I_{max}), and the remaining snowfall passes through the canopy. Snow in the canopy (I_s) may sublimate, melt, or unload. (b) Loading may be parameterized as a function dependent on I_{max} or not, and loading capacity may or may not increase with temperature. (c) Unloading may be a function of air temperature (T_{air}) and wind or may be a constant rate proportional to intercepted snow. (d) Branches clipped to a pole in the Rocky Mountains (Schmidt & Gluns, 1991). (e) Douglas firs in weighing lysimeters in the Oregon cascades (Storck, 2000)

Both snow stored under the canopy and land surface albedo matter to society, and calculations of both are influenced strongly by how a model represents both the capacity of snow to accumulate in the canopy and the rate, timing, and mechanism(s) of how that snow is removed from the canopy. In addition to increasing albedo, the longer snow stays on the canopy, the longer there is time for canopy snow to sublimate, which can result in about 20%–50% of the winter precipitation returning to the atmosphere (Lundberg & Halldin, 2001; Pomeroy & Schmidt, 1993; Sexstone et al., 2018). Snow lasting longer in the canopy also has more time to melt, resulting in liquid water that may not be stored in the underlying snowpack. Consequently, outside of high wind environments (e.g., Revuelto et al., 2015), over most of the snow accumulation season in forested environments, canopy interception is the primary driver of spatial variability of snow on the ground (Mazzotti et al., 2019). Total seasonal snow in the canopy can be increased by either increasing interception loading capacity, decreasing melt and drip rates of canopy snow, decreasing sublimation, or decreasing unloading, requiring that these processes be examined together.

Here, we review the literature to explain the history and epistemology of snow interception modelling (Section 2), including the origin and evolution of algorithms in current models and the original observations on which they are based. We focus specifically on loading and unloading in the context of weather and climate, leaving issues of forest structure as a subject for future work. We re-examine the observational literature in a global context to assess which process representations are most supported by field and laboratory data to provide recommendations and key hypotheses for testing. We employ a simple model of interception at two sites with different mean winter temperature and humidity (Section 3) to illustrate how model representations lead to different estimates of snow accumulation under forest cover and, more importantly, to different temperature sensitivities, to establish priorities regarding essential observations for validation and needed model modifications to adequately represent responses to forest and climatic change (Section 4). Finally, we outline a path forward for both observationalists and modellers to ensure a more holistic approach to understanding and modelling combined forest–snow–climate change (Section 5).

2 | HISTORY OF SNOW INTERCEPTION MODELLING

2.1 | Basic formulations and concepts

Most models take a similar form for the basics of interception (Table 1). When snow falls from the sky, some fraction of it is intercepted by the forest canopy, up to some maximum amount that the given canopy can hold, while the remaining fraction falls to the ground below (Figure 1). The snow in the canopy may sublimate or fall beneath or adjacent to the canopy. The canopy snow may also melt, in which case it may evaporate, drip to the ground below, and/or lubricate the remaining canopy snow so that some mixture of melted

and solid snow falls to the ground below. Key parameters involved in modelling these processes include interception efficiency, I_e (the fraction of snowfall intercepted at each timestep), the maximum interception, I_{max} , the sublimation rate, S , the melt rate of intercepted snow, M , and the unloading rate, U . In most models, these are some function of leaf area index, LAI , and/or fractional forest cover, which represent how much canopy cover is present. Some models explicitly represent the canopy energy balance and phase changes within it, while others parameterize conceptually how snow behaves within the canopy (Table 1). We focus here on interception efficiency, maximum interception, sublimation, melt, and unloading, with canopy structure left as a subject for future research.

2.2 | Model family trees

While significant earlier work existed observing and quantifying snow interception (Section 2.3), Hedstrom and Pomeroy (1998), hereafter referred to as HP98, were arguably the first to develop a coherent system of equations for modelling all of the processes involved and have influenced many models developed in subsequent years. Here we review their work in the context of the literature as a whole, highlighting parallel developments and diverging ideas.

2.2.1 | Interception

HP98 defined the interception rate as a function asymptotically approaching zero as total interception approaches I_{max} ,

$$dI_s/dt = (I_{max} - I_s) \left(1 - e^{-C_l P_s \Delta t / I_{max}} \right) / \Delta t, \quad (1)$$

where I_s is the intercepted snow per unit area, I_{max} is the maximum possible intercepted snow, P_s is snowfall, t is time, and C_l is the canopy leaf contact area per unit ground area. This function stemmed from prior work by Sattarlund and Haupt (1967), who weighed a Douglas-fir and a western white pine sapling (each ~4 m high) during two storms in northern Idaho, showing an increase and then levelling off of intercepted snow amounts over the course of these storms. Sattarlund and Haupt presented a conceptual understanding that interception rates start low (when there was no snow in the tree), increase as initial snowflakes bridge gaps between the needles, and then decrease again as falling ice crystals bounce off and as branches bend sufficiently for snow to fall off, essentially approaching the maximum interception capacity. This representation is referred to as a sigmoidal efficiency curve. Only the decrease in efficiency as I_s approaches I_{max} was preserved in HP98's formulation, making it an exponential, rather than sigmoidal, function. The maximum value was modelled as

$$I_{max} = \alpha(0.27 + 46/\rho_s) LAI, \quad (2)$$

TABLE 1 Canopy interception representations in commonly used hydrologic land surface models, as well as a selection of snow models

	CRHM	VISA	CLASS	UEB	VIC/DHSVM	SUMMA	Noah-MP	JULES	CLM	SnowModel	FSM	AMUNDSEN
Tracks canopy snow temperature				✓								
Models melt of intercepted snow		✓		✓	✓	✓	✓	✓				✓
Interception efficiency asymptotes to 0 as $I \rightarrow I_{max}$ (exponential function)	✓	✓	✓	✓	✓	✓	✓	✓	✓	✓	✓ ^{Mazzotti}	✓
Interception efficiency asymptotes to 0 as $I \rightarrow I_{max}$ (sigmoidal function)											✓ ^{Moeser}	
I_{max} function of density as defined by temperature	✓	✓	✓	✓		✓	✓					
I_{max} increases with temperature above -3°C					✓	✓						
Unloading exponential function of time	✓			✓		✓					✓ ^{Mazzotti}	
Unloading at temperatures at or above 0°C	✓	✓	✓	✓	✓	✓	✓	✓	✓	✓	✓	✓
Full unloading	✓											
Partial unloading ($f(T_{air})$) near or above 0°C	✓	✓	✓	✓	✓	✓	✓	✓	✓	✓	✓	✓
^b Unloaded as all solid	✓	✓	✓			✓ ^a				✓	✓	✓
^a Unloaded as mix (solid and liquid)				✓	✓	✓		✓				
Unloading as a function of wind speed						✓ ^a	✓					
Sublimation modelled based on the rate of loss from an ice sphere	✓									✓		✓
Sublimation modelled as a function of the wind profiles through the canopy, vapour pressure gradients, and aerodynamic resistance terms		✓	✓	✓	✓	✓	✓	✓	✓		✓ ^{Mazzotti}	
Sublimation modelled as a function of incoming solar radiation											✓ ^{Moeser}	

Note: For each process, ✓ = yes, included, and blank indicates not included. Model citations are as follows: CRHM (Pomeroy et al. 2007; Ellis et al. 2010); VISA (Niu & Yang, 2004); CLASS (Bartlett et al., 2006; Bartlett & Verseghy, 2015); UEB (Mahat & Tarboton, 2014); VIC & DHSVM (Andreadis et al., 2009); SUMMA (Clark et al., 2015); Noah-MP (Niu et al., 2011); JULES (Best, 2011; Essery et al., 2003); CLM (Lawrence et al., 2019); SnowModel (Liston & Elder, 2006); FSM (Essery, 2015; Mazzotti, Essery, Moeser, & Jonas, 2020; Moeser et al., 2015, 2016); AMUNDSEN (Strasser et al., 2007, 2011).

^aOnly in SUMMA 3.0 and later (<https://github.com/NCAR/summa>), not in the original. Note that SUMMA is a modular model framework and could be set up with or without these parameters.

^bVIC, DHSVM, and JULES unload snow at 40% of the canopy snowmelt rate. Others unload independently of melt rate (or without allowing melt to occur).

where LAI is the leaf area index, α is recommended to be 6.6 and 5.9 km m^{-2} for pine and spruce following Schmidt & Gluns (1991), and the fresh snow density in kg m^{-3} is estimated by

$$\rho_s = 67.92 + 51.25e^{(T_{\text{air}})^{2.59}}, \quad (3)$$

where T_{air} is air temperature ($^{\circ}\text{C}$).

The hard-coded parameters (0.27 and 46) in Equation (2) are based on fitting a curve to snow interception on branches at the two study sites in Schmidt and Gluns (1991): Fraser Experimental Forest, CO, winter 1989, and Nelson, British Columbia, Canada, winter 1990. At both locations, approximately 30 cm long branches of different tree species (Engelmann spruce, subalpine fir, and lodgepole pine, Figure 1(d)) were attached to a horizontal steel rod about 1 m above the snow surface. After each storm period, the snow was shaken off each branch and into a plastic bag, which was weighed. Total snowfall was estimated from what accumulated on an adjacent snow board. Schmidt and Gluns (1991) mentioned greater cohesive forces at temperatures between -3 and 0°C multiple times (discussed further below), but these comments were not translated into equations or functional forms in HP98's model development, likely because temperatures in this range would play a very minor role in the cold continental climate of Saskatchewan, Canada.

The fresh snow density numbers (Equation (3)) are based on storm total snow board measurements from the two sites in Schmidt and Gluns (1991) (their table 2), as well as from observations from the Central Sierra Snow Laboratory in California (USACE, 1956, their plate 8-1, their fig. 4). Note that the observations were taken over storm-

total time periods, which varied in duration but were generally 6 h or longer, while the model equation is typically applied at hourly timesteps. Due to the complexity of processes witnessed, both studies report the relationship as likely highly uncertain, and subsequent studies have found air temperature to be a poor predictor of new snowfall density (e.g., Wayand et al., 2017, their fig. 7). These equations have gone on to be used in a number of land surface models (Table 1 and Figure 2), including VISA (Niu & Yang, 2004), Noah-MP (Niu et al., 2011), CLM (Lawrence et al., 2019), and CLASS (Bartlett et al., 2006; Bartlett & Verseghy, 2015).

The concept of a maximum interception load appears in all models (Table 1). The sigmoidal form (Satterlund & Haupt, 1967), of slow initial interception rates that increase with time, only reappears in a recent development of FSM (Essery, 2015), with application by Moeser et al. (2015), but was later removed from FSM by Mazzotti, Essery, Webster, et al. (2020). Additionally, the influence of temperature and snow cohesion on interception, while dropped in HP98, reappeared in an independent line of snow model development (Figures 1(b) and 2), described in Andreadis et al. (2009) and used in the VIC and DHSVM models. Their basic interception model is based on two winters in the Oregon Cascades, where two full sized Douglas Firs were weighed on load cells (Storck, 2000, Figure 1(d)). Temperatures at this site hovered near 0°C all winter, but Storck (2000) noted that during one cold storm when temperatures were less than -5°C , the maximum interception decreased by a factor of 4. Andreadis et al. (2009) combined this observation with the results of Kobayashi (1987), who found that between -3 and 0°C , the cohesion of ice increases, leading to increased interception on boards. Thus,

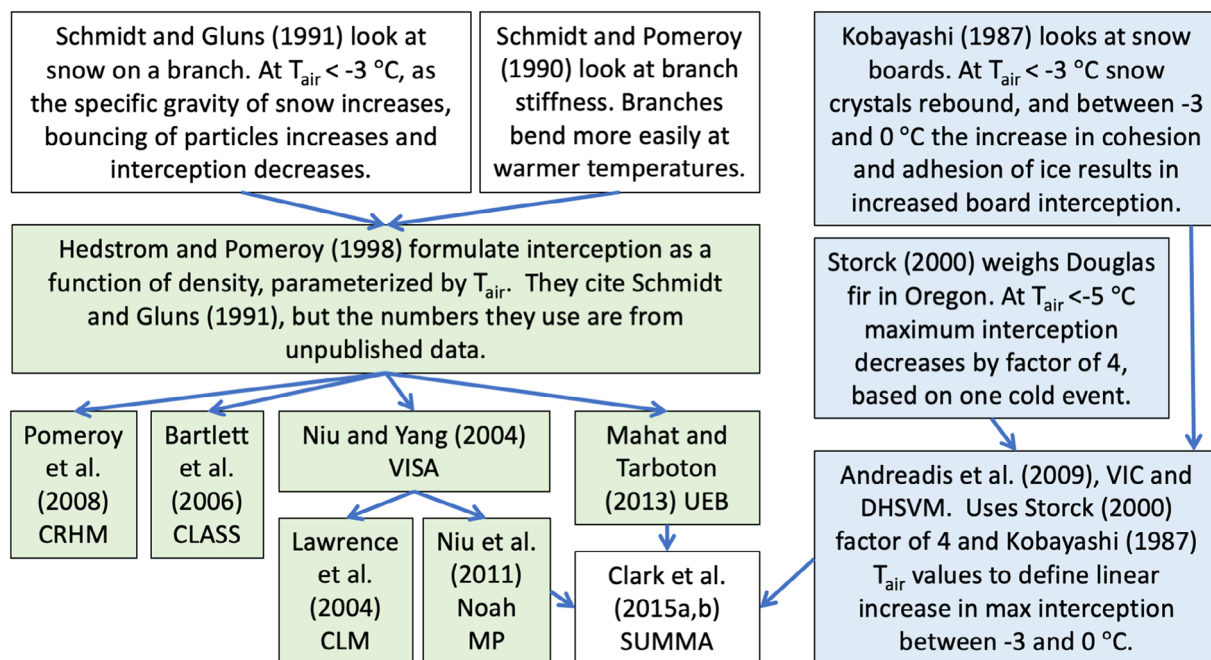


FIGURE 2 Flow path of model development between the Hedstrom and Pomeroy versus Andreadis I_{max} formulations shown in Figure 1. Models listed in green boxes employ the solid red line in Figure 1(b) (and formulas 2 and 3), while models listed in the blue boxes employ the black dashed line in Figure 1(b) to model maximum interception as a function of temperature

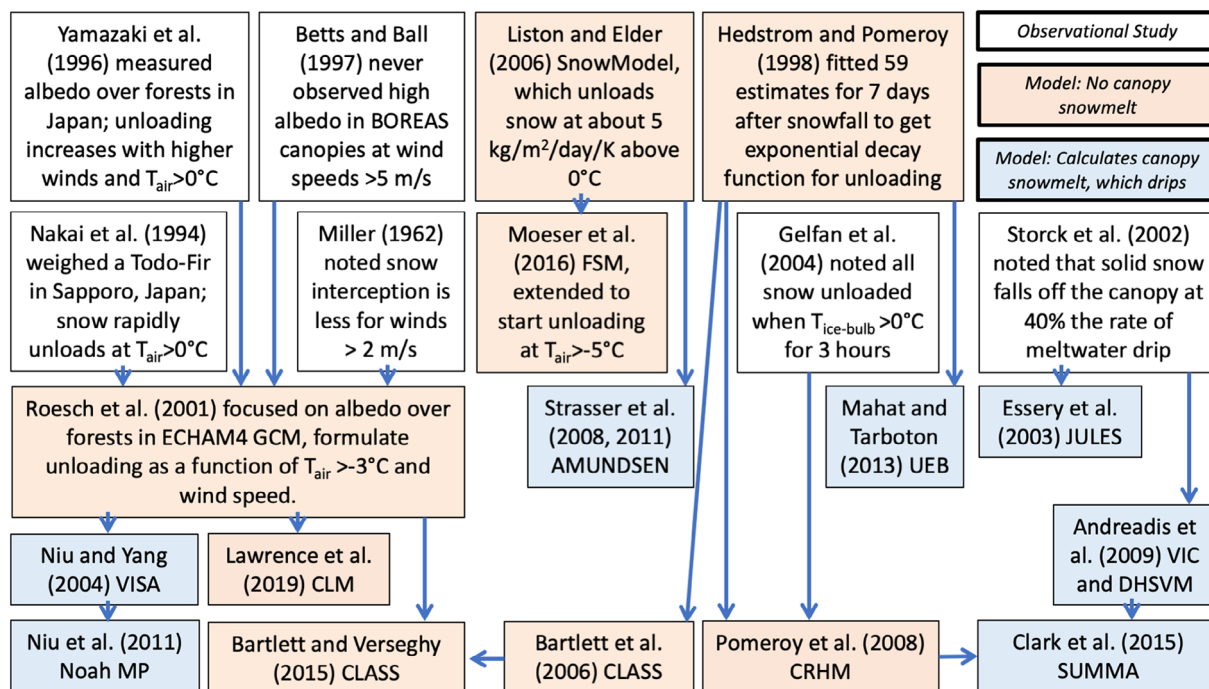


FIGURE 3 History of model development for snow unloading. Arrows indicate flow of information through paper citations, while blue colors represent models that calculate snowmelt, which is then lost from the canopy through melt water drip, and orange colors indicate models that do not calculate canopy snowmelt. White boxes are observational studies and not models

they modelled the maximum snow interception as increasing linearly between -3 and 0°C by a factor of 4.

To summarize, interception processes in almost all current land surface models can be traced back to the evolution of interception efficiency in two storms in Idaho, which helped inform Equation (1) in HP98. The value of I_{max} in these models was determined by the behaviour of branches attached to a steel rod, or by comparing one cold interception event to average conditions in Oregon combined with a study on boards, with the decision between the two approaches depending primarily on which specific research groups and other modelling papers a given model stemmed from (Figures 1 and 2). While the originating studies all examined evergreen conifers in mountains, the two study areas had very different climates (maritime vs. continental), with different temperature regimes.

2.2.2 | Unloading

While maximum snow accumulation in interception models follows either HP98 or Storck, 2000 (Figure 2), representations of unloading of canopy snow are more varied (Figure 3). Given their differing foci on relatively cold (HP98) and warm (Storck, 2000) environments, HP98 described snow unloading from a tree as an exponential function of time, approaching zero over a few days, while Storck (2000) observed frequent unloading whenever temperatures rose above zero. Illustrated on the right side of Figure 3, Storck et al. (2002) quantified the ratio of solid snow mass release to meltwater drip to be 0.4, and this formulation was incorporated by Essery et al. (2003) in JULES

and by Andreadis et al. (2009) in VIC and DHSVM. Pomeroy's further development of the HP98 model in CRHM added an additional term, based on work by Gelfan et al. (2004), wherein all snow was unloaded from the canopy in solid form when ice-bulb temperatures remained above freezing for 3 h in the presence of wind speed greater than 0.5 ms^{-1} , but not all models using the equations of HP98 added this modification (Figure 3). A third line of reasoning originated with Roesch et al. (2001), who were trying to improve albedo representations over the boreal forest in the ECHAM4 GCM and disagreed with the premise of HP98 that intercepted snow would approach zero simply as a function of time. Drawing on four observational studies with general descriptions of how snow unloads at higher wind speeds and at temperatures greater than -3°C , they formulated unloading to be a fraction of the existing intercepted snow, with the fraction varying with the observed wind speed and canopy air temperature relative to threshold values. These functions were adopted by multiple land surface models in the years following, including VISA (Niu & Yang, 2004), Noah MP (Niu et al., 2011), and CLASS (Bartlett & Verseghy, 2015), as well as in the migration of CLM4.5 to CLM5.0 (Lawrence et al., 2019; Perket, 2015), (Figure 3). Liston and Elder (2006), in developing SnowModel, unloaded snow as a function of air temperatures greater than 0°C but did not include wind-related unloading. Mazzotti, Essery, Moeser, and Jonas (2020), in FSM2, implemented exponential decay unloading as in HP98, but with different time constants for cold versus melting snow conditions. Note that model decisions about whether to calculate canopy snowmelt (and subsequent meltwater drip) appear to be made independently of decisions about snow unloading (Figure 3, Table 1), with the exception of models deriving

from Storck et al. (2002), which directly relate solid snow unloading to dripping melt water.

2.2.3 | Sublimation

Due to greater winds and solar exposure, as well as larger exposed snow surface area, sublimation from the canopy is larger than sublimation from the forest floor. Because canopy sublimation only occurs when snow is in the canopy, total sublimation is directly linked to the duration snow stays in the canopy. In all land surface models and most snow models, sublimation increases with increasing wind speed and with decreasing atmospheric humidity (Table 1). Wind speed is scaled as a function of canopy height, using either exponential or logarithmic profiles. Two general families of formulas exist (Table 1). In CRHM, SnowModel, and AMUDSEN, sublimation is calculated based on laboratory experiments (Thorpe & Mason, 1966), which related the sublimation rate of individual ice spheres to relative humidity and wind speed. This is then modified to include the additional influence of solar radiation absorbed by the particle as developed for a blowing snow model (Schmidt, 1972), and scaled based on studying snow on an artificial tree (Schmidt, 1991) and a fractal analysis of photographs of snow on boreal forest branches (Pomeroy & Schmidt, 1993). In most land surface models, the formulas used for sublimation closely follow the model's representation of canopy evaporation. VISA, CLASS, UEB, VIC, DHSVM, SUMMA, CLM, JULES, Noah-MP, and the latest version of FSM all calculate sublimation based on bulk aerodynamic formula. While models adjust for stability conditions differently, see Lapo et al. (2019) for review, sublimation scales with wind speed and with vapour pressure gradients in all but the rare representations of stable conditions shutting down turbulence completely. We leave a full analysis of canopy wind speed variations and stability corrections as a subject for future research.

2.3 | Recommendations based on published observations

Measurements of canopy snow interception are difficult (see Friesen et al. (2015) for a review of techniques), but many more direct measurements exist than appear to have been used in model development. Here, we review these observations to determine in which aspects they agree with current modelling practices for interception and unloading, and in which aspects they suggest changes are necessary.

2.3.1 | Interception efficiency

Interception efficiency reaching 0 when total interception approaches a specific I_{max} is not supported from collective observational evidence. Satterlund and Haupt (1967) originated the idea of sigmoidal interception efficiency with time, reaching a maximum interception value. This function was based on earlier work on the interception of liquid

precipitation (Merriam, 1960). After hanging and weighing two 4 m high saplings (Douglas Fir and White Pine) for one month in Priest River, Idaho in a clearing sheltered from the wind, their data showed that after snow initially fell on the tree, the interception rate increased rapidly and then levelled off (Figure 4(a)). They described the levelling off as the capacity of the tree to retain snow.

While most models include the idea that interception efficiency approaches zero as a maximum interception value is approached, no published dataset examining conifers, other than Satterlund and Haupt's, fits this form better than it would fit a constant interception efficiency (Figure 4). Often only one or a few data points that appear to indicate a maximum interception are used to justify the maximum. Data from both Switzerland and France (Helbig et al., 2020, their fig. 5) show near constant interception efficiency over a range of snowfall amounts. The exception is Moeser et al. (2015), who showed an initially increasing and then decreasing interception efficiency over nine storms in Switzerland. Observations from the Nothofagus forests of the Southern Andes (Huerta et al., 2019) suggest that the models of both Hedstrom and Pomeroy (1998) and Moeser et al. (2016) consistently underestimated the largest interception events, which would indicate their decrease in interception efficiency was not supported in the Nothofagus forests.

Separately, observations in Japan show accumulated snow depth on boards of different widths flattens out only for the heaviest snowfall and not for cases of moderate snowfall (Shidei, 1952) (translation can be found on page 119, fig. 7.21 in Bunnell et al., 1985). Using spatial measurements in Hokkaido, Japan, Lundberg et al. (2004) found that the snowfall fraction intercepted and lost to sublimation varied strongly with forest sky view fraction but had no relationship with snowfall magnitude.

Throughout the literature, the raw data present a question: Is there a stable maximum interception capacity which influences interception efficiency? The presence of a stable maximum interception amount, pervasive in our modelling, may not be the best fit for the data available (Figure 4(b)–(f)). The discrepancy may be due, at least in part, to the difference between a canopy system, which often has multiple layers of branches, including those overlapping from adjacent trees, and an isolated hung sapling, or to the aggregation of multiple storms versus a presentation from one specific storm sequence. It could be due to a belief that there ought to be a maximum carrying capacity, irrespective of whether there is evidence in the available data, or to the true carrying capacity being so large (e.g., the point where a tree breaks) that measuring it is impractical. Another explanation could be that the apparent maximum is reached when unloading rates equal interception rates, although this equilibrium would likely be quite variable between trees, storms, and so forth. A final consideration is how different functional forms of this equation affect model stability. We explore these questions further in Section 3.

2.3.2 | Changing snow cohesion and adhesion

Changing snow cohesion and adhesion with temperature is a well-documented physical process. The efficiency of snow interception is a

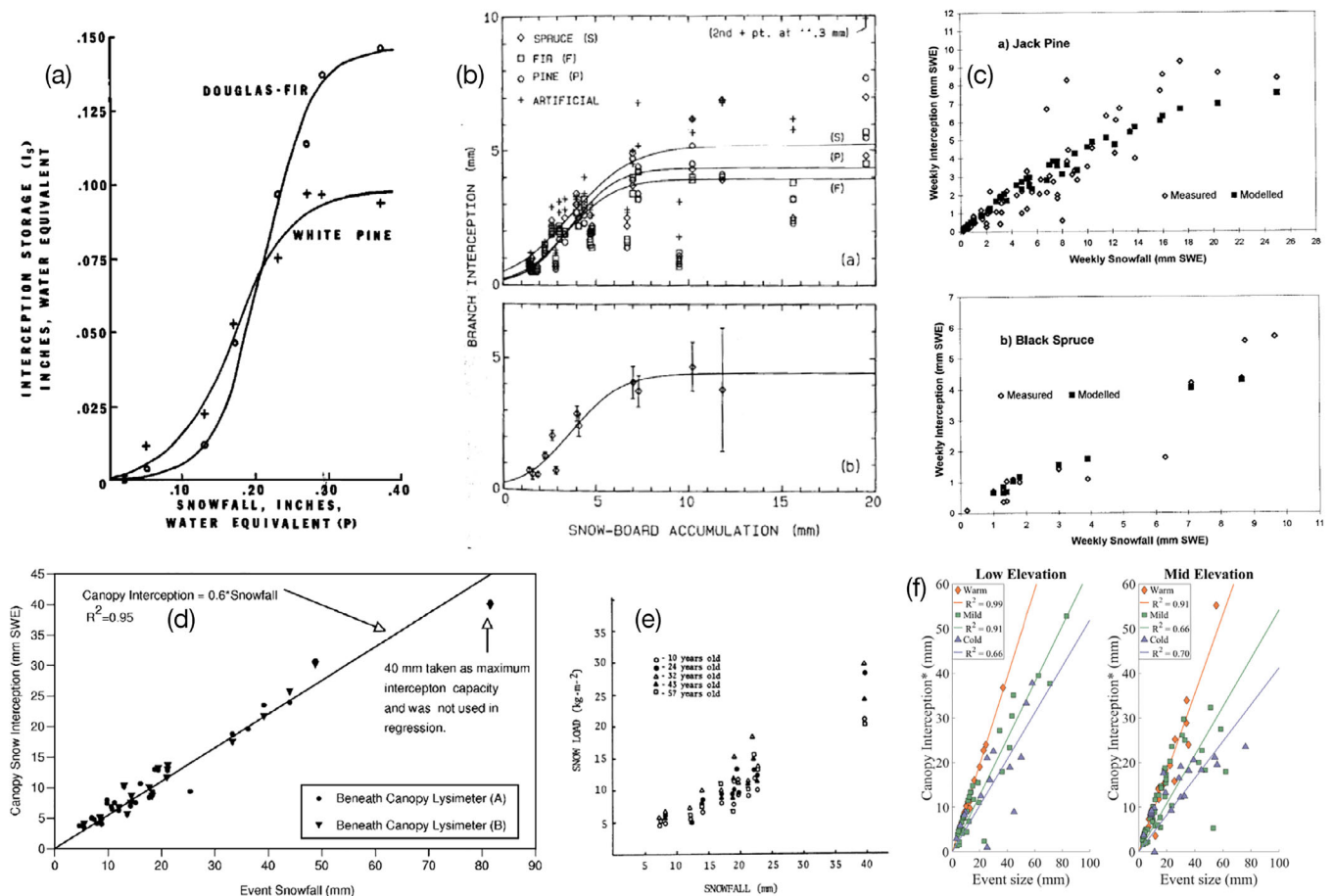


FIGURE 4 (a) From Satterlund and Haupt (1967)'s fig. 2, curves for two saplings for one storm event; (b) from Schmidt and Gluns (1991)'s fig. 4, note large scatter of points around drawn curves as well as notation of a point off the top of the plotting range; (c) from Hedstrom and Pomeroy (1998)'s fig. 6, note that modelled (filled squares) level off but that measured (diamonds) diverge from the model at high values; (d) from Storck (2000)'s fig. 5.4, note single point taken as I_{max} , which does not diverge much from a linear fit; (e) from Watanabe and Ozeki (1964), as translated in Bunnell et al. (1985), their fig. 7.31; (f) from Roth and Nolin (2019)'s fig. 5, note lack of any data suggesting a levelling off at I_{max}

function of adhesion and cohesion countered by elastic rebound. The cohesion between snow crystals increases between the temperatures of -3 and 0°C , and this increased cohesion increases snow interception (Bunnell et al., 1985). The angle of repose of a pile of snow crystals increases rapidly at temperatures above -3.5°C , approaching nearly vertical at temperatures near 0°C (Kuroiwa, 1967). Increased interception with warming temperatures has been observed on boards (Kobayashi, 1987; Pfister & Schneebeli, 1999; Shidei, 1952), when weighing trees (Shidei, 1952; Storck, 2000) and through comparing snow accumulation under trees and nearby clearings after storms (Dickerson-Lange et al., 2017; Roth & Nolin, 2019). Quasi-liquid layers are apparent on ice at temperatures slightly below 0°C (Sazaki et al., 2012), and these facilitate increased growth rates of bonds between snow crystals. Any sequence of events leading to a thin film of water present on the trees or previously intercepted snow before snow falls leads to the greatest adhesion and hence, the greatest interception efficiency (Bunnell et al., 1985; Shidei, 1952).

Schmidt and Gluns (1991) found that elastic rebound, that is, bouncing, is greater for snow with higher specific gravity, but they

also wrote, "Greater specific gravity is associated most often with warm storms, where cohesive forces reduce elastic rebound." Similarly, Filhol and Sturm (2019) found that colder crystals bounced more, but that crystal type mattered as well as temperature. In general crystal type is also a function of air temperature (Libbrecht, 2019; Nakaya, 1954). At temperatures between -3 and 0°C , snow crystals generally form dendrites and plates, which adhere and form aggregates more readily than needles and columns, which form at temperatures between -10 and -3°C (Nakaya, 1954). Below -10°C , dendrites form again, but at these colder temperatures, cohesion is much less (Nakaya, 1954). The total range of solid precipitation types possible at temperatures near 0°C , from crystals to ice pellets to freezing rain, is diverse and complex (Stewart et al., 2015). Even HP98, whose functional form of I_{max} (Figure 1) indicates the opposite, noted, "There is a slight trend for greater interception efficiency at higher temperatures."

To summarize, all of our physical understanding and empirical evidence indicates that the air temperature during snowfall is a predicting variable of the efficiency at which snow is intercepted by

the canopy. To a first order, some representation of increased interception efficiency with temperatures rising between -3 and 0°C , should be included in all land surface models. To further improve, some representation of the impact of temperatures prior to storm on the canopy (cold vs. warm enough to have a thin film of liquid water), as well as the cloud physics and meteorology leading to the crystal type, could be included. However, using the concept of I_{max} , which in some models changes with temperature (Figure 1), may not be the best approach, as examined in Section 3.

2.3.3 | Snow unloading

Wind and warmer temperatures control the rate and timing of unloading snow and should be included in modelling. Despite its use in many models, no observational data are presented in the literature that support snow unloading as predominantly an exponential decay function of time. This functional form may be used as a proxy for other processes but has no empirical or physical basis. Rather, the literature supports wind removing 33%–100% of the snow load in cases of dry and cold snow without near-melt layers to bond it (Bunnell et al., 1985; Goodell, 1959; Hoover & Charles, 1967); in many cases, wind also limits the net amount of snow intercepted during colder storms, likely due to unloading happening simultaneously with interception. The effect of wind on decreasing interception is greater when branches (or boards, as tested) are at steeper angles (Shidei, 1952).

Rainfall and temperatures warming above 0°C are also common causes of snow unloading. Satterlund and Haupt (1970) report that most frequently snow was “washed off of the trees by rain.” While the correlation in timing of warm temperatures and unloading is frequently reported in the literature and is represented in the majority of models (Table 1 and Figure 3), many models do not calculate melt for intercepted snow in the canopy. Thus, many unload all snow in a solid form, even at air temperatures greater than 0°C . Quantifying how much intercepted snow is unloaded as solid snow versus meltwater is difficult, and reports range from drip being “uncommon” in California (Kittredge, 1953) to “constant” in Oregon (Miller, 1962). Satterlund and Haupt (1970) stated that only 5% of the intercepted snow became liquid meltwater drip. Miller (1966) postulated that the “the release of intercepted snow occurs after 20% of it has melted” based on examination of the timing and likely energy input to snow observed by studies weighing a tree in Japan (Shidei, 1952). Storck (2000) derived the conclusion that 40% of liquid meltwater drip falls as solid snow based on careful comparisons of adjacent lysimeter readings in the open and under the forest during two different 2 week periods in December of each year when there was neither rain nor melting of ground snow. Storck (2000) advised that the consistency of a 40% ratio across only two carefully chosen study periods was more of a hypothesis to be further tested than a conclusive value. Thus, while energy available for melt, as indicated by warmer temperatures, is clearly associated with unloading, the form (solid or liquid) of that unloaded water is less clear. Unloaded solid snow adds mass to

the underlying snowpack, while unloaded liquid water may refreeze in the underlying snowpack, be retained as liquid water in the underlying snowpack, or pass through the snow to contribute immediately to soil moisture and/or runoff.

3 | METHODS: FORMULATING IMODEL

To better understand which model parameters and processes have the largest impact on model output, we investigate how different model interception configurations impact both snow accumulation under the canopy and snow duration in the canopy. Because the duration snow stays in the canopy impacts the likelihood that intercepted snow will sublimate or melt, and hence not contribute to accumulation, these processes are closely linked.

While all existing models have a maximum interception parameter, the collective data supporting this is not clear (Section 2.3.1). Also, while interception efficiency should increase with temperature (Section 2.3.2), incorporating this may not make a large difference in model performance, particularly if unloading depends on temperature. For example, Niu et al. (2011) illustrated Noah-MP simulations that match the dataset from Storck (2000) well, despite using formulations primarily derived from HP98 (Figure 2).

To determine which model choices have the greatest impact on model results, we formulate the experimental interception model, iModel, which has two state variables: intercepted snow in the canopy (I_s) and snow under the canopy (SWE_u). The model can be configured with a set maximum interception value (I_{max}), such that $I_e = f(I_s, I_{max})$, I_{max} constant, or with a variable maximum interception value, $I_e = f(I_s, I_{max}, I_{max} = f(T_{air}))$. For both of these, the time evolution of intercepted snow is defined by

$$\frac{dI_s}{dt} = \left[(I_{max} - I_s) \left(1 - e^{-\left(\frac{P_s}{I_{max}}\right)} \right) \right] - S - I_s \left(M_T \frac{T_{air}}{C_T} + M_V \frac{U}{C_V} + M_{td} C_{td} \right) - M_{fac} T_{air}, \quad (4)$$

where I_e is interception efficiency, P_s is snowfall, I_{max} is the maximum interception capacity, S is sublimation rate, T_{air} is air temperature, U is wind speed, C_T and C_V are coefficients for rates of unloading with temperature and wind, respectively, as in Roesch et al. (2001) and Niu et al. (2011). C_{td} is the rate of exponential-decay unloading, as in Hedstrom and Pomeroy (1998), and M_{fac} is the melt rate as a function of degrees C above 0°C . Each unloading formula has a multiplier coefficient (M_T , M_V , M_{td}) so that the process may be turned off or rates may be modified. The constant I_{max} is set at the minimum value in Table 3, while the variable I_{max} scales linearly between temperatures of -3 and 0°C , such that it equals the minimum value at -3°C or lower temperatures and reaches the minimum plus the scale factor at 0°C (Table 3).

The sublimation rate is calculated as

$$S = C_{sub} U (e_{ss} - e_a), \quad (5)$$

where C_{sub} is a parameter, e_{ss} is the vapour pressure above the canopy snow, assumed to be the saturation vapour pressure over ice at the smaller of air temperature or 0°C, and e_a is the atmospheric vapour pressure, calculated as a function of air temperature and relative humidity using the Magnus-Tetens formula (Murray, 1966) with coefficients from Alduchov and Eskridge (1996), as described in Feld et al. (2013).

The interception efficiency may also be configured without a maximum interception value, with either a constant efficiency (I_e constant, no I_{max}), or an interception efficiency that varies with temperature ($I_e = f(T_{air})$, no I_{max}). In this case the time evolution of intercepted snow is described by:

$$\frac{dl_s}{dt} = I_e P_s - S - I_s \left(M_T \frac{T_{air}}{C_T} + M_V \frac{U}{C_V} + M_{td} C_{td} \right) - M_{fac} T_{air}, \quad (6)$$

with variables and parameters defined the same as for (4). Thus, the model allows us to investigate canopy loading configurations, with or without dependence on temperature or maximum interception, while also testing their sensitivity to unloading rates and configurations, through changing their multipliers.

Snow below the canopy accumulates as a function of snowfall that is not intercepted plus unloaded solid snow from the canopy. Melt is not calculated for subcanopy snow. Liquid water falling from the canopy is presumed to pass through the subcanopy snowpack without contributing to subcanopy SWE. This is a fair assumption in warm maritime regions like the U. S. Pacific Northwest, where frequent rain on snow results in a saturated and isothermal snowpack with flow channels through it (Pflug et al., 2019). However, the model may underestimate subcanopy SWE in cases when a deep subcanopy snowpack stores liquid water and may refreeze the water. We examine this in more detail in Section 5.2.

The model uses the Matlab ordinary differential equation solver, ode15s, which starts with initial conditions of 0 snow in the canopy and then compares the results of first and fifth order Runge-Kutta methods to determine the error and appropriate timestep (Shampine & Reichelt, 1997). This approach allows for directly solving differential Equations (4) and (6), given the dependence of changes in intercepted snow on the snow currently in the canopy.

Atmospheric forcing data are drawn from 1997 to 1998 observations at Umpqua, OR, described in Storck (2000) and from 2008 to 2009 observations at the Swamp Angel site at Senator Beck, CO,

TABLE 2 Study site meteorology for 1 December to 1 April

Site	Analysis water year	Mean air temperature (°C)	Total precipitation (mm)	Mean relative humidity (%)	Mean wind speed (m s ⁻¹)	Potential melt (mm)	Potential sublimation (mm)
Umpqua, OR	1997–1998	0	639	92	1.5	392	116
Senator Beck, CO (Swamp Angel)	2008–2009	-7	533	65	1.2	205	961

Note: Potential melt and sublimation were calculated using the baseline model parameters and equations, assuming there was always canopy snow available to melt or sublimate.

Name	Units	T-wind unloading	Exponential-decay unloading
M_T	-	0.25	0
M_V	-	0.25	0
M_{td}	-	0	1
$I_{e\min}$	mm	0.6 ^(a)	
$I_{e\text{scale}}$	mm°C ⁻¹	0.4 ^(b)	
$I_{max\min}$	mm	20 ^(c)	
$I_{max\text{scale}}$	mm°C ⁻¹	65 ^(c)	
M_{fac}	mm°C ⁻¹ h ⁻¹	4/24 ^(d)	
C_{sub}	mm Pa ⁻¹ m ⁻¹ s	0.002 ^(e)	
RScutoff	°C	1.5 ^(f)	
C_T	s ⁻¹	1.87×10^5 ^(g)	
C_V	s ⁻¹	1.56×10^5 ^(g)	
C_{td}	s ⁻¹	1.2861×10^{-6} ^(h)	

Note: Rain falling at temperatures below the rain-snow cutoff (RScutoff) is assumed to be all snowfall, with all rainfall above. Source: Sources for parameter values: (a) Storck (2000); (b) Andreadis et al. (2009); (c) Martin et al. (2013), see their tab. 1 for maximum measured intercepted snow in different climates; (d) Raleigh and Lundquist (2012); (e) Lundberg and Halldin (2001); (f) Lundquist et al. (2008); (g) Roesch et al. (2001); (h) Mahat and Tarboton (2014).

TABLE 3 iModel parameter settings

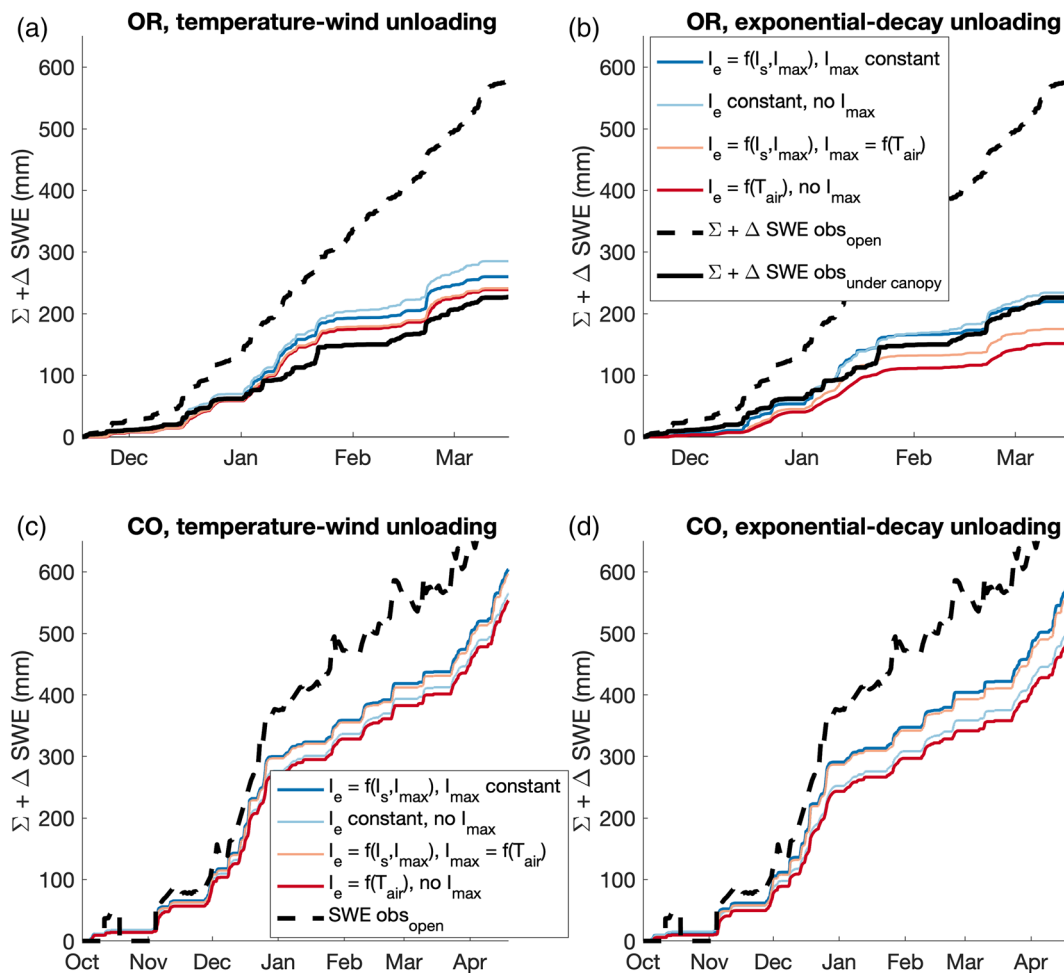


FIGURE 5 Timeseries of (a,b) modelled, with default parameters in Table 3, and observed snow accumulation on the ground under the canopy for Umpqua, OR for water year 1997–1998 and (c,d) for Swamp Angel, Senator Beck, CO for water year 2008–2009. Columns refer to unloading schemes, while colors refer to loading configurations. Warmer colors representing interception schemes with greater interception amounts at warmer temperatures. Snow accumulation ($\Sigma + \Delta \text{SWE}$) is represented by the cumulative sum of SWE increases, available for the Oregon site from a weighing lysimeter. Actual SWE is shown for the Colorado site, which, because little melt occurred during this period, matches well with modelled cumulative SWE in the open

described in Landry et al. (2014). The Oregon data include 2 h observations of precipitation, air temperature, relative humidity, and wind, as well as weighing measurements of snow water equivalent (SWE) under the canopy, in the open, and in three trees. This location is chosen because of its high-quality observations and warm winter temperatures, to which we expect our model variations to be sensitive. The Colorado data include hourly observations of precipitation, air temperature, relative humidity, and wind, as well as observations of snow in a forest clearing. The clearing SWE timeseries is a function of combining continuous snow depth measurements with density from periodic snow pit observations. This location was chosen as a colder and drier site for comparison of model sensitivities to changing temperatures; however, note that there are no under-canopy snow observations for this site. Mean values for the December 1–April 1 period during each site's analysis year are detailed in Table 2.

Model simulations were designed not to pick the best configuration but rather, to illustrate the relative sensitivity to different model choices in two different environments. Observations from Oregon were used to benchmark model performance and select reasonable baseline model parameters from the literature (Table 3). Using this fixed set of parameters, we examined the impact of changing the model's representation of loading and unloading on the timeseries of cumulative snow water equivalent added to the subcanopy snowpack (Figure 5) and the timeseries of intercepted snow in the canopy (Figure 6). We then examined the impact of doubling ($2C_{sub}$) and halving ($0.5C_{sub}$) sublimation, not allowing snow to melt in the canopy ($M_{fac} = 0$), and halving the rate of exponential unloading ($0.5M_{td}$), for each of the loading and unloading schemes. These simulations were each repeated across a range of temperatures, by uniformly increasing or decreasing air temperature to adjust the mean December to March temperature to range from -7°C (which was observed at the

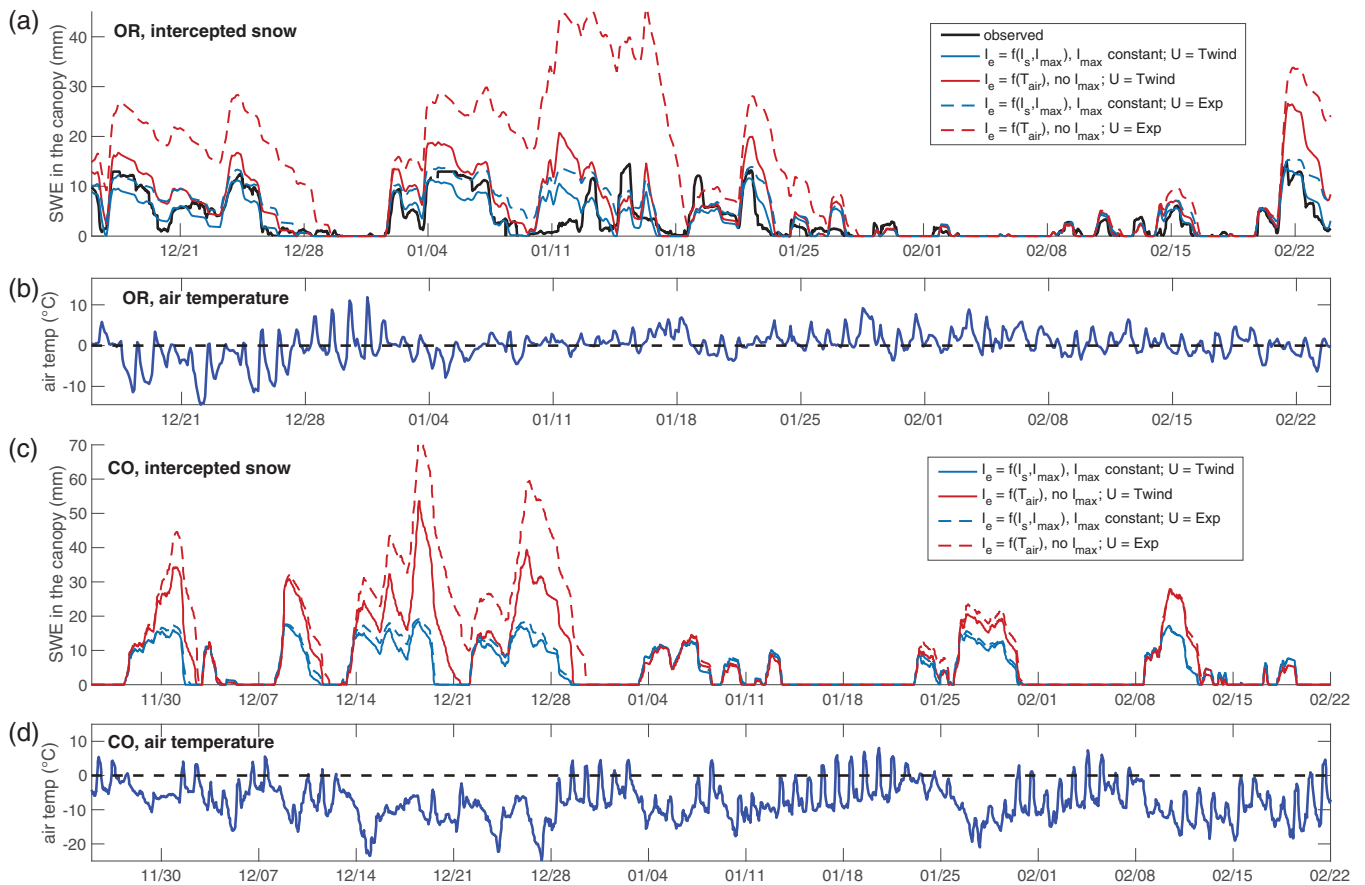


FIGURE 6 Intercepted snow (a) and temperature (b) for 1997–1998 at Umpqua, OR and (c,d) for 2008–2009 at Senator Beck, CO (subset of time-periods shown in Figure 5), where colored lines refer to the loading schemes as in Section 3, and line styles represent variations in canopy unloading. Model parameters are for baseline simulations in Table 2. The black line (a) shows intercepted snow from a ponderosa pine tree cut and weighed on a lysimeter

Colorado site) to 0°C (which was observed at the Oregon site). This range represents modelled snow evolution at colder or warmer sites experiencing the same sequence of weather events, for example, as might be expected at nearby higher or lower elevations. In these scenarios, total precipitation and relative humidity are held fixed, but the fraction of precipitation falling as snow and the vapour pressure are adjusted with temperature. The modelled temperature sensitivity is compared to literature values.

For each simulation, the fraction of snow below the canopy compared to the open is calculated as the ratio of total model snow accumulated over the season (subcanopy:open), neglecting melt. The ground observations at the Oregon site, from a weighing lysimeter, were also presented as the cumulative sum of positive changes in SWE, neglecting melt, following the approach of Dickerson-Lange et al. (2017). The implications of neglecting melt are discussed further in Section 5.2. The fraction of time snow is in the canopy is calculated as the total timesteps with model intercepted snow greater than 0.5 mm divided by the total model timesteps during the evaluation period. For Oregon, this period encompassed 18 November 1997 to 7 April 1998 (the duration of measurements), while for Colorado this period encompassed 1 October 2008 to 30 April 2009 (the duration of snowfall events).

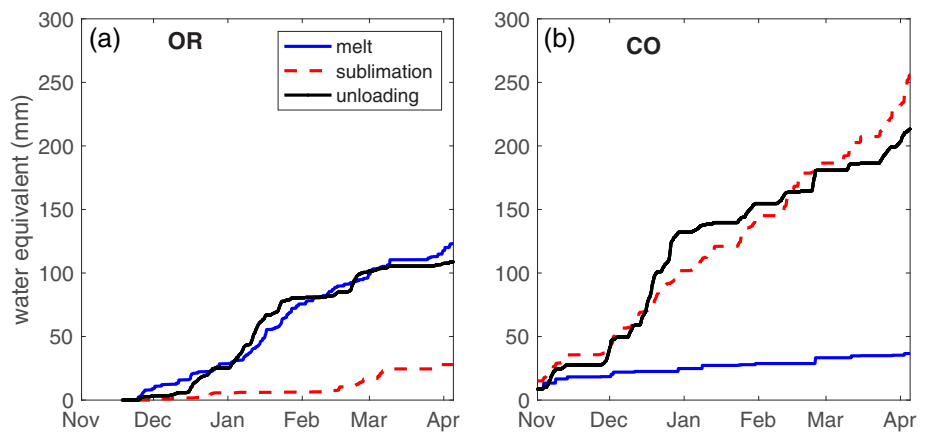
4 | IMODEL RESULTS

4.1 | Comparisons to timeseries of observational data

With the baseline parameter set (Table 3), both temperature-based unloading and exponential-decay unloading schemes were able to simulate below canopy snow accumulation (Figure 5(a),(b)) and intercepted snow (Figure 6(a)) close to observed values at Umpqua, OR. The loading schemes with interception efficiency a function of air temperature (red and orange lines) performed better with temperature-wind unloading (Figures 5(a) and 6(a)), while the loading schemes with a constant l_{max} (blue lines) performed better with exponential decay unloading (Figures 5(b) and 6(a)). In Colorado, within canopy and subcanopy observations were not available, but the same model configurations showed sensitivity to the different climate, with snow under the canopy in Colorado accumulating about 65% of that in the open, compared to only about 40% accumulating subcanopy in Oregon (Figure 5).

At the Oregon site, the two simulations with loading dependent on air temperature grouped more closely together, whereas at the Colorado site, the two simulations with l_{max} grouped more closely together (Figure 5). In all cases, the simulations with $l_e = \text{constant}$, no

FIGURE 7 Cumulative losses of snow water equivalent from the canopy for (a) Umpqua, OR and (b) Senator Beck, CO, for the baseline simulation using the temperature-wind unloading parameterization and the loading scheme of $l_e = f(T_{air})$ and no l_{max}



l_{max} and with $l_e = f(l_s, l_{max})$, $l_{max} = f(T_{air})$ fell close to or in between the other two loading schemes. Therefore, for clarity in visualization, only simulations with $l_e = f(l_s, l_{max})$, $l_{max} = \text{constant}$ and with $l_e = f(T_{air})$, no l_{max} are shown in subsequent plots. In the interception timeseries for Colorado (Figure 6(c)), the temperature-dependent loading schemes were indistinguishable from those with no temperature dependence because snow almost never fell in the -3 to 0°C temperature range (Figure 6(d)). The choice of loading scheme produced the largest variation in canopy SWE when coupled with exponential-decay unloading (Figure 6(c)). At both locations, the model simulations with l_{max} led to similar interception timeseries with both exponential and temperature-wind unloading schemes, but over twice as much snow accumulated in the canopy when the simulation with no l_{max} was coupled with the exponential unloading scheme (Figure 6(a),(c)).

Beyond different temperature regimes and sensitivities to loading schemes, the two sites varied in the modelled fate of intercepted snow (Figure 7). The warm and moist Oregon site has very little sublimation, as the relative humidity was close to 100% during times when snow was in the canopy, but the amount of snow melting from the canopy was comparable with that unloading. In contrast, the colder and drier Colorado site had comparable sublimation and unloading from the canopy, with less snow melting. This affected the relative sensitivity of each site to changing model parameters related to melt and sublimation, as discussed in the next section.

4.2 | Model sensitivity to parameter change and temperature change

As illustrated with the timeseries (Figures 5 and 6), multiple model configurations can produce similar results at a single site, with similar timing of snow in the canopy. However, the maritime (OR) and continental (CO) sites had different fates of that intercepted snow (Figure 7) and different fractions of snow accumulating beneath the canopy compared to the open (Figure 5). To investigate the model's sensitivity to changing parameters and temperatures in these two different climates, we ran the model at both sites with uniform temperature offsets ranging from -7 to 0°C at the Oregon site and from 0 to $+7^\circ\text{C}$ at the Colorado site, such that the weather timeseries at each was adjusted towards the mean

winter temperature at the other. The range of parameters and loading/unloading schemes discussed in Section 3 illustrate a range of reasonable results that might be expected from existing land surface models. The results provide an indication of the uncertainty in simulations performed at a given temperature and with perturbed temperatures, which is one measure of model transferability.

For each simulation and mean December–March temperature, we consider the fraction of snow water equivalent accumulating below the canopy compared to the open and the fraction of time snow is in the canopy (Figure 8). Observations at the Oregon site fell within the range of the simulations that included canopy melt, but the simulations without canopy melt were far from observations. At the Colorado site, simulations without melt fell within the range of those with melt, indicating that this was a less sensitive model choice at this site.

With mean Dec–Mar temperatures of -7°C , the relative amount of snow accumulating below the canopy depends both on the time that snow stays in the canopy and the sublimation rate, such that simulations with more time to sublimate and/or more rapid sublimation lose more snow to the atmosphere, with the subcanopy:open snow accumulation ratio varying by up to 30%. At these temperatures, the lack of canopy snowmelt does not affect the fraction, since temperatures are not warm enough to melt snow at times snow is in the canopy. The drier Colorado site has greater sensitivity to modelled sublimation rates and thus a wider spread in subcanopy snow fraction. As illustrated in Figure 7, a factor of 2 increase in sublimation at the Colorado location would make total sublimation substantially more than unloading, whereas a factor of two increase in sublimation in Oregon would still leave total sublimation less than half of unloading. The fraction of time snow is present in the canopy varies up to 15% at either site and is a function of the amount of loading and the combined rates of loss (to sublimation and/or melt) and unloading.

As mean Dec–Mar temperatures approach 0°C , not only does the total snow on the ground decrease, but the relative fraction of snow below the canopy compared to the open decreases for most simulations (Figure 8(a), (c)), as has also been documented in the literature (Dickerson-Lange et al., 2017; Roth & Nolin, 2019). Excluding the no-melt simulations, the Oregon site was more sensitive to temperature change than the Colorado site (Figure 8), with decreases in the ratio of snow subcanopy ranging from -17% to -39% (about a 20% range).

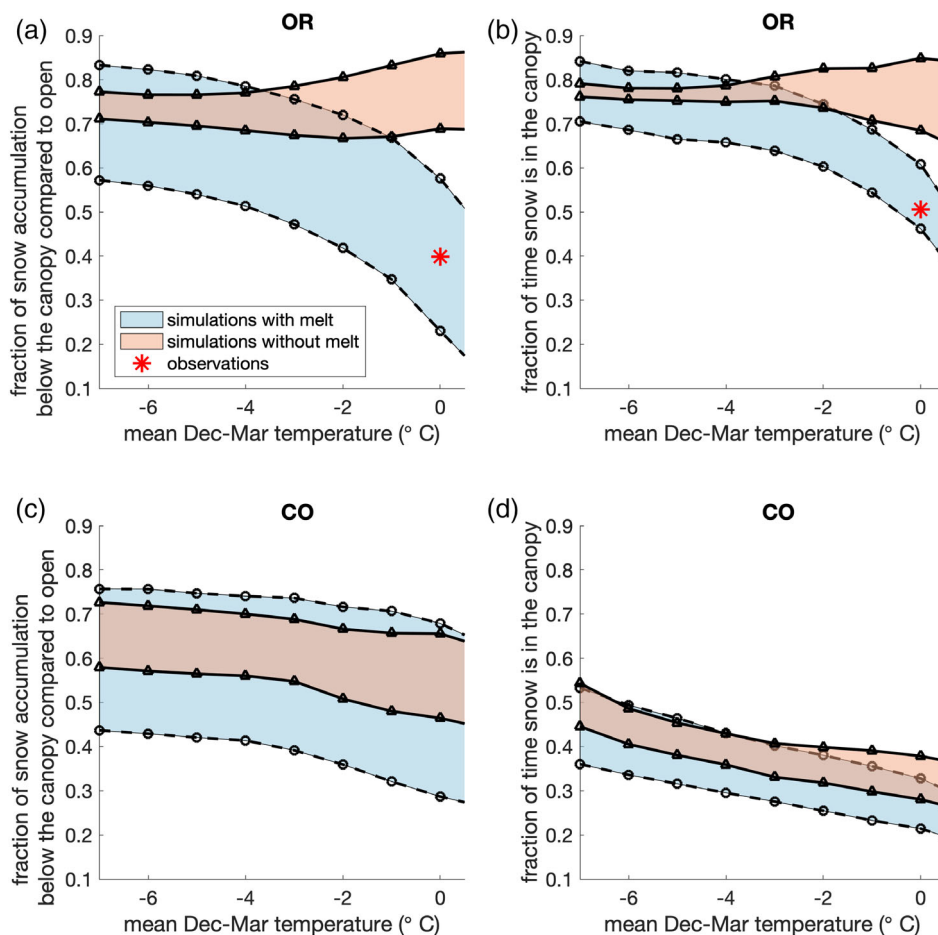


FIGURE 8 Temperature change sensitivity for (a,b) Umpqua, OR for water year 1997–1998 and for (c,d) Senator Beck, CO for water year 2008–2009 for multiple model configurations with regards to (a,c) the fraction of seasonal-total snow accumulating under the canopy compared to the open and (b,d) the fraction of time when snow is present in the canopy. For reference, observed mean temperature for Oregon was 0°C and for Colorado was -7°C , so in general, Oregon temperatures were cooled while Colorado temperatures were warmed to compare results assuming similar mean temperatures. The fractions observed at the Oregon site are plotted at the observed mean temperature

In contrast, for the Colorado simulations, the ratio of snow subcanopy decreased by -7% to -17% (about a 10% range) with 7°C warming. The temperature sensitivity at the Colorado site was driven by increases in sublimation, as the water vapour pressure gradient increased when air temperatures warmed above 0°C , but the snow surface temperature was capped at 0°C . Thus, while simulations with no canopy melt showed slightly less sensitivity to warming temperatures, all model simulations at the Colorado site exhibited decreases in both relative snow below the canopy and fraction of time snow is in the canopy. Because of the minimal amount of sublimation at the maritime site (Figure 7), the climate sensitivity results from intercepted snow melting and dripping instead of unloading in solid form. For these warm temperatures with an isothermal subcanopy snowpack, drip results in a loss of water from the snow system. Simulations without canopy melt were unable to represent these key processes.

5 | DISCUSSION

5.1 | Model sensitivities and indications for experimental design

The model simulations at Umpqua, OR and Senator Beck, CO illustrate both the relative order of importance of model decisions for two

locations and the importance of considering multiple climates. In these simulations, the model decision with the greatest impact on model sensitivity to temperature change was the choice to allow canopy snow to melt (Figures 8 and 9), which is currently included in about half of land surface models (Figure 3; Table 1). However, this result only appeared when modelling at the maritime site with mean winter temperatures near 0°C . Colder and/or drier climates lose more snow to sublimation than to melt (Figure 7), and research focused on these regions would not likely identify canopy melt as a process critical to hydrology. However, forest cover is extensive in many maritime snow zones, such as the Pacific Northwest of the U.S., the Coast Mountains of western Canada, and much of Japan, and these regions are loci of some of the largest divergence in snow simulations across multi-model ensembles (Kim et al., 2020). Given that most models are intended to simulate snow responses to changes in weather and climate globally, appropriately representing canopy melt is essential.

The model choice with the greatest impact on the fraction of subcanopy snow accumulation compared to the open at a specific mean winter temperature was the sublimation rate (Figure 9), which had a greater impact in conjunction with the unloading scheme because snow lasting longer in the canopy sublimated more. These impacts were much greater at the drier Colorado site. Unlike canopy melt, which is a known process that could simply be added to model code, sublimation is extremely difficult to measure, and the physics leading

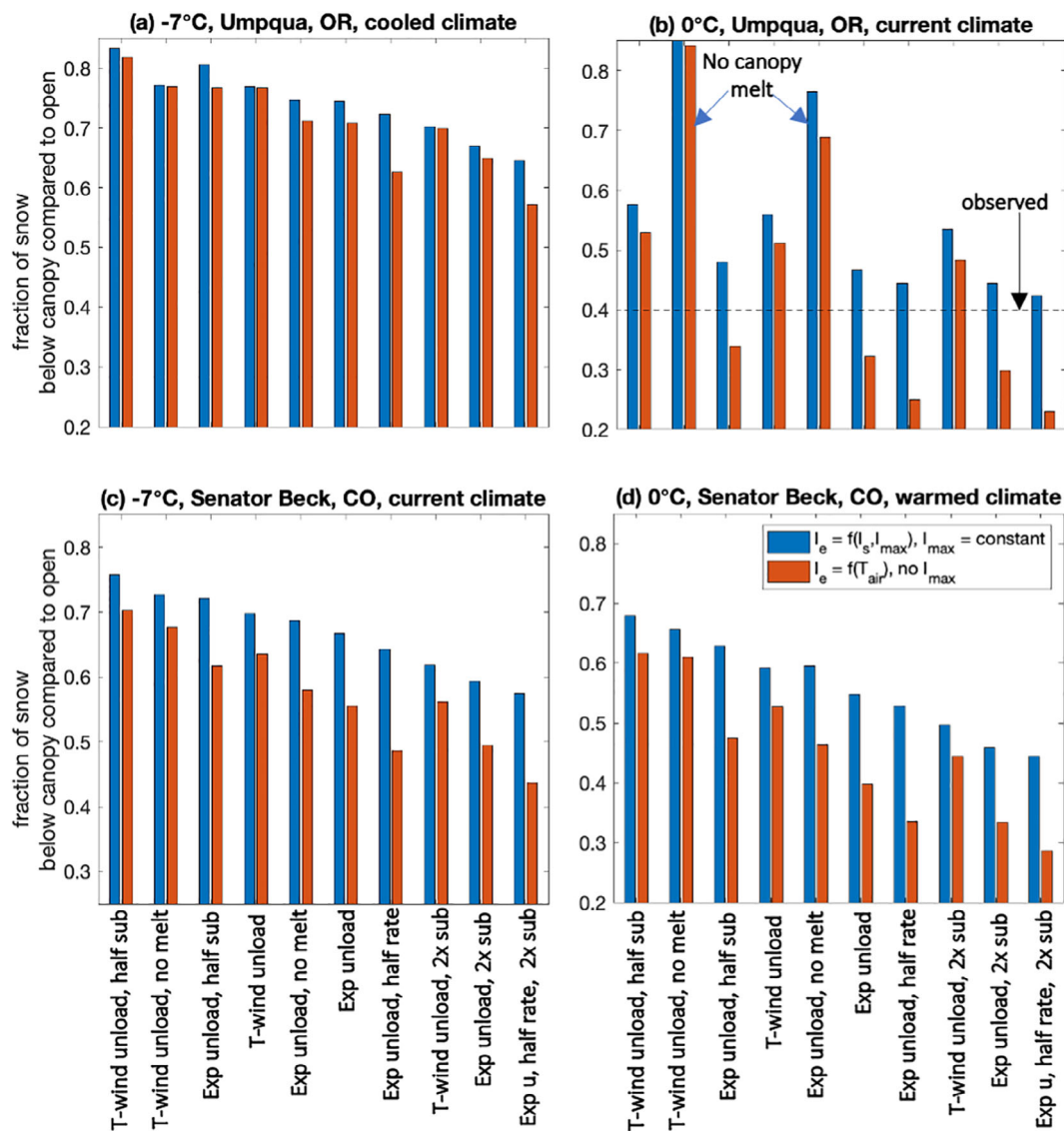


FIGURE 9 Fraction of snow below the canopy compared to the open, as in Figure 8, but specifying specific run values at mean December to March temperatures of -7°C (observed at the CO site) and at 0°C (observed at the Oregon site). The value observed at the Oregon site is marked with a horizontal dashed line in (b)

to variations in sublimation rates, such as the influence of stability and wind fields through forests, are still an active area of study and debate (LeMone et al., 2019).

The choice of model loading scheme was equally as important as the choice of model unloading scheme (Figure 9), but the best choice of one was dependent on the choice of the other (Figures 5 and 6). While comparing our model simulations to observations at one site was not sufficient to declare any loading/unloading scheme superior, the literature review suggests that temperature-based loading and unloading is supported by observations and physical understanding. While the combination of loading to a fixed I_{max} and exponential unloading matches observations well (Figures 5(b) and 6(a)), it may prove less transferable once more observations are available.

Simulations employing loading schemes with interception efficiency a function of air temperature had greater sensitivity to

changing temperatures (Figure 9). This greater sensitivity is supported by the literature. In the Pacific Northwest, a 3°C average winter temperature increase across multiple sites corresponded with an observed 50% decrease in the under-forest: open peak snow accumulation (Dickerson-Lange et al., 2017, their fig. 3). A 40% decrease in this ratio was observed between cold and warm storms which differed by $\sim 6^{\circ}\text{C}$ at sites in Oregon (Roth & Nolin, 2019, their fig. 4). Over 30 years of observations in the boreal forest of Northern Sweden showed that the ratio of snow under the forest compared to the open has declined about 20% (Kozii et al., 2017). They found that the best explanations for this variation were that the amount of precipitation falling at temperatures less than -3°C led to more similar forest: open ratios, and that the number of total days with temperatures above $+0.4^{\circ}\text{C}$ led to lower forest: open ratios. Thus, their work also supports the conclusions here that interception efficiency increasing above -3°C , and

melt and sublimation losses increasing above 0°C, are important processes to represent in models to adequately simulate sensitivity to temperature changes.

5.2 | Canopy melt, drip, and subcanopy snow

As formulated, iModel does not add liquid melt water to the snow below the canopy, and thus, whether the model simulates canopy snowmelt or simply unloads solid snow directly impacts the subcanopy SWE accumulation. Meltwater from the canopy has been observed refreezing in the snowpack in some environments (Teich et al., 2019), so by not allowing meltwater drip to add to subcanopy SWE, iModel may be overestimating the hydrologic impact of melting canopy SWE.

However, the degree of this overestimation is a function of the environment, and the assumption that melt water generally passes through the snowpack is fair at warm maritime sites similar to the Oregon site simulated here. Sites with large oscillations in temperature, such as periods of melt following periods with air temperatures substantially below 0°C, often have cold and dry snowpacks that are capable of incorporating canopy melt through increasing residual water content and/or refreezing. In contrast, warmer maritime sites frequently experience rain on snow, resulting in saturated and isothermal snowpacks. Observations show that under these conditions liquid water drains from the snowpack in less than a day, often at snowpack densities less than would be assumed from observations in colder climates, leading to a lack of transferability of some model representations of snowpack liquid water percolation (Pflug et al., 2019). When analyzing errors in snow accumulation modelling in maritime regions, a significant source of error arises from partitioning precipitation into rain versus snow (Wayand et al., 2016, 2017). The model choice to melt canopy snow or unload it in solid form would similarly impact the model evolution of subcanopy SWE.

Here, we deliberately focused on subcanopy:open SWE accumulation ratios, neglecting the influence of melt and not plotting actual SWE on the ground. Lundquist et al. (2013) discussed the importance of midwinter melt in removing subcanopy snow in regions with warm winters and plotted (their fig. 4) how the relative differences in subcanopy to open snow gain versus loss contributed to differences in peak SWE on the ground. For 1997–98 at Umpqua, OR, the same data examined here, peak SWE on the ground was 222 mm in the open compared to 50 mm under the forest (Lundquist et al., 2013). Of this, 131 mm of the difference could be attributed to accumulation differences, while only 52 mm could be attributed to melt differences, with 11 mm of snow in the open lost during a period when no snow was on the ground under the forest. These results suggested that while greater midwinter melt occurs under the canopy than in the open, snow lost through interception processes accounts for a larger fraction of the difference. Dickerson-Lange et al. (2017) followed up by examining paired observations of snow in the forest and under canopies across the Pacific Northwest and found that throughout the region, differences in snow accumulation explained the bulk of

seasonal differences in both peak SWE and snow duration. Given the high humidity and low sublimation in the maritime region, the only way these observations can occur is for canopy snow to melt, and for the meltwater to pass through the snow below the canopy, not contributing to subcanopy SWE accumulation.

Thus, we argue that all models should include canopy melt to accurately represent subcanopy snow in warm maritime environments. Our results are not sufficient to argue the importance of this representation in other environments, which may explain why the family tree of models that include canopy melt (Figure 3) consists primarily of models that have included the Oregon dataset in their evaluation. In regions outside the maritime Pacific Northwest, observations of snow stratigraphy and density in adjacent forest-covered and open areas show that snow composition and the range of observed snow density under forests is clearly more variable than in an adjacent opening (Teich et al., 2019). However, under-canopy snow is not consistently more or less dense (Broxton et al., 2019, see their supplemental material). Therefore, the fate of melting canopy snow and under-forest snow evolution warrants further study.

5.3 | Order of operations, model stability, and time-stepping schemes

Often unloading happens during interception events, particularly in colder storms with high winds or in warmer storms when snowfall changes to rain. While loading and unloading are two separate processes, data often contain both, and models may solve an ordinary differential equation (ODE) with adaptive timesteps and near-simultaneous adjustments of both loading and unloading, as we have here, or may have a set order of operations, such that unloading may only be allowed after an interception event. With this in mind, our concept that interception efficiency decreases over time might simply be an effect of simultaneous unloading. There is also a chance that within-storm unloading is accounted for twice in the model: first, by way of an erroneously reduced interception efficiency, and again by way of the unloading function. Numerical details are seldom reported in papers and are beyond the scope of this work. However, we encourage anyone working on interception model development to pay particular attention to the coding of the processes.

5.4 | Canopy structure

We have focused here on interception processes within a single tree or idealized canopy, neglecting the impact of canopy structure. Our existing interception datasets also weigh single trees or branches, and thus do not resolve canopy structure effects. However, moving forward, if we plan to use snow on the ground as an evaluation dataset for interception modelling, we must ensure that the evaluation is done in the context of a full energy and mass-balance model that represents canopy structural effects on the domain over which measurements take place (e.g., Mazzotti, Essery, Webster, et al., 2020 and references

therein). Beyond impacting snow on the ground, the canopy arrangement will also affect interception processes. Canopy elements with more solar exposure will lose intercepted snow first (either from sublimation or melting), and canopy elements with more wind exposure may either intercept more snow (e.g., preferential deposition of snowfall along downwind canopy edges or fog harvesting in riming conditions) or lose snow more rapidly (from wind unloading).

6 | CONCLUSIONS

Current global land surface representations of snow interception by forest canopies are based on a handful of observations from two locations. However, despite the similar observational basis, models vary in whether canopy loading capacity or efficiency increases with temperature, in whether or not they model canopy snow melt, and in how they represent unloading. Based on simulations varying these components, these differences lead to different estimates in how snow accumulation under the canopy compares to the open and different sensitivities regarding how snow in forested regions responds to changes in temperatures.

In the Northern Hemisphere winter, approximately 50% of the snow covered zone is forested (Kim et al., 2017). However, most ground observations of snow are located in forest clearings (Farnes, 1967), and current satellite remote sensing of snow cannot visibly see nor reliably measure snow under forests (Rittger et al., 2020; Vuyovich et al., 2014). Therefore, snow under a forest canopy must be estimated or modelled relative to snow observed in the open. Here, variations in interception processes alone led to sub-canopy snow accumulation ratios compared to the open that varied by 30%, suggesting that interception processes contribute to a large component of uncertainty in modelling the current hydrology of snow and forest-covered regions and in predicting the hydrologic response of these regions to forest or temperature change.

The literature review and modelling presented here reveal that there are ways to better constrain current model variations. Our analysis suggests, that, at a minimum, all model representations of snow interception should model snow melt in the canopy to accurately represent canopy effects in maritime regions. At the wet and warm Oregon location, simulations without canopy snow melt showed the least sensitivity to temperature and were unable to match observations of both snow in the canopy and snow beneath the canopy.

We further suggest that models should include a temperature-based representation of increased cohesion as snow approaches the melting point, which increases the canopy interception efficiency and/or capacity. Ample observational evidence demonstrates that snow cohesion increases as temperatures approach the melting point, leading to greater interception efficiency. Model simulations show that while any of the existing snow loading parameterizations can match a season of intercepted snow data, those with interception efficiency varying as a function of temperature show more sensitivity to temperature change, more closely matching variations reported in the literature.

The choice of modelling changes in interception efficiency (I_e) directly or in maximum interception efficiency (I_{max} , with I_e a function of I_{max}) led to differences in simulated snow, but these differences were smaller than most other changes tested. Therefore, we recommend not using I_{max} because it is an unnecessary model complication and is not supported in the literature (Figure 4), but if it is already built into a model, it is less important to update than the recommendations above. Similarly, either an exponential decay function or a physical basis for snow unloading (e.g., temperature and wind dependence) could replicate observations from Oregon. We recommend temperature and wind based unloading based on the observational literature and strongly recommend that model loading and unloading schemes be examined together and in the context of canopy sublimation and melt.

With the exception of a few studies (e.g., Hedstrom & Pomeroy, 1998; Storck, 2000), direct observations of snow interception have not been impressive in the years since the work in Japan in the 1950s and 60s (Shidei, 1952). More locations, with a range of forest types and climates, should be targeted for careful, detailed lysimeter and tree weighing work, accompanied by accurate atmospheric data to run and test land surface models of snow evolution. Such work should be accompanied by newer technology, such as time-lapse photography (Bartlett & Versegny, 2015) and lidar measurements of the forest (White et al., 2016) and the snow beside and beneath it (Deems et al., 2013). Constraining our estimates of snow under forest canopy depends on model improvement, and the evaluation of canopy interception processes and their representation is only possible with more observations.

ACKNOWLEDGEMENTS

Thank you to the Japanese government for supporting forest-snow research and to the British Columbia Ministry of Forestry for supporting translation of this work in the form of Bunnell's work. Thank you to the National Science Foundation Grant #CBET-1703663 for supporting the majority of our work on this synthesis, and to NASA Grant #80NSSC18K1405 for additional support. Thank you also to NCAR for a visiting scientist position in 2013–2014 and to the Swiss Federal Research Institute WSL for a visiting faculty fellowship in 2021 to Lundquist to support this work. Thank you further to the Swiss government for prioritizing keeping primary schools open during the Covid-19 pandemic and to the U.S. childcare providers who continued operating through the pandemic; without that support, I could not have finished this paper. NCAR is supported by the National Science Foundation.

DATA AVAILABILITY STATEMENT

The iModel code and datasets will be posted to the Mountain Hydrology GitHub site <https://github.com/Mountain-Hydrology-Research-Group/> by the end of 2021. Anyone with questions about the code or the literature included in the review is welcome to contact the first author, Jessica Lundquist, at jdlund@uw.edu.

ORCID

Jessica D. Lundquist  <https://orcid.org/0000-0003-2193-5633>

Susan Dickerson-Lange  <https://orcid.org/0000-0002-2157-4033>

Ethan Gutmann  <https://orcid.org/0000-0003-4077-3430>

Tobias Jonas  <https://orcid.org/0000-0003-0386-8676>

Cassie Lumbrazo  <https://orcid.org/0000-0003-1656-9771>

Dylan Reynolds  <https://orcid.org/0000-0001-5677-6092>

REFERENCES

- Adams, H. D., Guardioli-Claramonte, M., Barron-Gafford, G. A., Villegas, J. C., Breshears, D. D., Zou, C. B., Troch, P. A., & Huxman, T. E. (2009). Temperature sensitivity of drought-induced tree mortality portends increased regional die-off under global-change-type drought. *Proceedings of the National Academy of Sciences*, *106*(17), 7063–7066.
- Alduchov, O. A., & Eskridge, R. E. (1996). Improved Magnus form approximation of saturation vapour pressure. *Journal of Applied Meteorology and Climatology*, *35*(4), 601–609.
- Allen, C. D. (2009). Climate-induced forest dieback: An escalating global phenomenon. *Unasylva*, *231*(232), 60.
- Andreadis, K. M., Storck, P., & Lettenmaier, D. P. (2009). Modelling snow accumulation and ablation processes in forested environments. *Water Resources Research*, *45*, W05429. <https://doi.org/10.1029/2008WRO07042>.
- Bartlett, P. A., MacKay, M. D., & Verseghy, D. L. (2006). Modified snow algorithms in the Canadian land surface scheme: Model runs and sensitivity analysis at three boreal forest stands. *Atmosphere-Ocean*, *44*(3), 207–222. <https://doi.org/10.3137/ao.440301>
- Bartlett, P. A., & Verseghy, D. L. (2015). Modified treatment of intercepted snow improves the simulated forest albedo in the Canadian land surface scheme. *Hydrological Processes*, *29*(14), 3208–3226. <https://doi.org/10.1002/hyp.10431>
- Best, M. J. (2011). The joint UKland environment simulator (JULES), model description—Part 1: Energy and water fluxes. *Geoscientific Model Development*, *4*, 677–699.
- Bormann, K. J., Brown, R. D., Derksen, C., & Painter, T. H. (2018). Estimating snow-cover trends from space. *Nature Climate Change*, *8*(11), 924–928. <https://doi.org/10.1038/s41558-018-0318-3>
- Broxton, P. D., van Leeuwen, W. J. D., & Biederman, J. A. (2019). Improving snow water equivalent maps with machine learning of snow survey and lidar measurements. *Water Resources Research*, *55*(5), 3739–3757. <https://doi.org/10.1029/2018WRO24146>
- Bunnell, F. L., McNay, R. S., & Shank, C. C. (1985). *Trees and snow: The deposition of snow on the ground: A review and quantitative synthesis*. Province of British Columbia.
- Carlyle-Moses, D. E., & Gash, J. H. (2011). Rainfall interception loss by forest canopies. In *Forest hydrology and biogeochemistry* (pp. 407–423). Springer.
- Clark, M. P., Nijssen, B., Lundquist, J. D., Kavetski, D., Rupp, D. E., Woods, R. A., Freer, J. E., Gutmann, E. D., Wood, A. W., Gochis, D. J., Rasmussen, R. M., Tarboton, D. G., Mahat, V., Flerchinger, G. N., & Marks, D. G. (2015). A unified approach for process-based hydrologic modelling: 2. Model implementation and case studies. *Water Resources Research*, *51*(4), 2515–2542.
- Cristea, N. C., Lundquist, J. D., Loheide, S. P., II, Lowry, C. S., & Moore, C. E. (2014). Modelling how vegetation cover affects climate change impacts on streamflow timing and magnitude in the snowmelt-dominated upper Tuolumne Basin, Sierra Nevada. *Hydrological Processes*, *28*(12), 3896–3918. <https://doi.org/10.1002/hyp.9909>
- Deems, J. S., Painter, T. H., & Finnegan, D. C. (2013). Lidar measurement of snow depth: A review. *Journal of Glaciology*, *59*(215), 467–479. <https://doi.org/10.3189/2013JG12J154>
- Dickerson-Lange, S. E., Gersonde, R. F., Hubbart, J. A., Link, T. E., Nolin, A. W., Perry, G. H., Roth, T. R., Wayand, N. E., & Lundquist, J. D. (2017). Snow disappearance timing is dominated by forest effects on snow accumulation in warm winter climates of the Pacific northwest, United States. *Hydrological Processes*, *31*(10), 1846–1862.
- Ellis, C. R., Pomeroy, J. W., Brown, T., & MacDonald, J. (2010). Simulation of snow accumulation and melt in needleleaf forest environments. *Hydrology and Earth System Sciences*, *14*(6), 925–940.
- Essery, R. (2015). A factorial snowpack model (FSM 1.0). *Geoscientific Model Development*, *8*(12), 3867–3876. <https://doi.org/10.5194/gmd-8-3867-2015>
- Essery, R., Pomeroy, J., Parviainen, J., & Storck, P. (2003). Sublimation of snow from coniferous forests in a climate model. *Journal of Climate*, *16*(11), 1855–1864. [https://doi.org/10.1175/1520-0442\(2003\)016<1855: Soslcf>2.0.Co;2](https://doi.org/10.1175/1520-0442(2003)016<1855: Soslcf>2.0.Co;2)
- Farnes, P.(1967). *Criteria for determining mountain snow pillow sites*. Paper presented at the Proceedings of the 35th Annual Western Snow Conference
- Feld, S. I., Cristea, N. C., & Lundquist, J. D. (2013). Representing atmospheric moisture content along mountain slopes: Examination using distributed sensors in the Sierra Nevada, California. *Water Resources Research*, *49*(7), 4424–4441. <https://doi.org/10.1002/wrcr.20318>
- Filhol, S., & Sturm, M. (2019). The smoothing of landscapes during snowfall with no wind. *Journal of Glaciology*, *65*(250), 173–187. <https://doi.org/10.1017/jog.2018.104>
- Friesen, J., Lundquist, J., & Van Stan, J. T. (2015). Evolution of forest precipitation water storage measurement methods. *Hydrological Processes*, *29*(11), 2504–2520.
- Gelfan, A., Pomeroy, J., & Kuchment, L. (2004). Modelling forest cover influences on snow accumulation, sublimation, and melt. *Journal of Hydrometeorology*, *5*(5), 785–803.
- Goodell, B. (1959). *Management of forest stands in western United States to influence the flow of snow-fed streams*. Association internationale d'hydrologie scientifique.
- Halofsky, J. E., Peterson, D. L., & Harvey, B. J. (2020). Changing wildfire, changing forests: The effects of climate change on fire regimes and vegetation in the Pacific northwest, USA. *Fire Ecology*, *16*(1), 4. <https://doi.org/10.1186/s42408-019-0062-8>
- Hedstrom, N., & Pomeroy, J. (1998). Measurements and modelling of snow interception in the boreal forest. *Hydrological Processes*, *12*(10–11), 1611–1625.
- Helbig, N., Moeser, D., Teich, M., Vincent, L., Lejeune, Y., Sicart, J. E., & Monnet, J. M. (2020). Snow processes in mountain forests: Interception modelling for coarse-scale applications. *Hydrology and Earth System Sciences*, *24*(5), 2545–2560. <https://doi.org/10.5194/hess-24-2545-2020>
- Hoover, M. D., & Charles, F. (1967). *Leaf, 1967*. Paper presented at the process and significance of interception in Colorado subalpine forests. In International Symposium on Forest Hydrology. Oxford and New York.
- Huerta, M. L., Molotch, N. P., & McPhee, J. (2019). Snowfall interception in a deciduous *Nothofagus* forest and implications for spatial snowpack distribution. *Hydrological Processes*, *33*(13), 1818–1834. <https://doi.org/10.1002/hyp.13439>
- Kim, E., Gatebe, C., Hall, D., Newlin, J., Misakonis, A., Elder, K., Marshall, H. P., Heimstra, C., Brucker, L., De Marco, E., Crawford, C., Kang, D. H., & Entin, J. (2017). *NASA's SnowEx campaign: Observing seasonal snow in a forested environment*. Paper presented at the 2017 IEEE International Geoscience and Remote Sensing Symposium (IGARSS).
- Kim, R. S., Kumar, S., Vuyovich, C., Houser, P., Lundquist, J., Mudryk, L., Durand, M., Barros, A., Kim, E. J., Forman, B. A., Gutmann, E. D., Wrzesien, M. L., Garnaud, C., Sandells, M., Marshall, H.-P., Cristea, N., Pflug, J. M., Johnston, J., Cao, Y., ... Wang, S. (2021). Snow Ensemble Uncertainty Project (SEUP): quantification of snow water equivalent uncertainty across North America via ensemble land surface modeling. *The Cryosphere*, *15*(2), 771–791. <http://dx.doi.org/10.5194/tc-15-771-2021>.
- Kittredge, J. (1953). Influences of forests on snow in the ponderosa-sugar pine-fir zone of the Central Sierra Nevada. *Hilgardia*, *22*(1), 1–96.
- Kobayashi, D. (1987). Snow accumulation on a narrow board. *Cold Regions Science and Technology*, *13*(3), 239–245.

- Kozii, N., Laudon, H., Ottosson-Löfvenius, M., & Hasselquist, N. J. (2017). Increasing water losses from snow captured in the canopy of boreal forests: A case study using a 30 year data set. *Hydrological Processes*, 31(20), 3558–3567. <https://doi.org/10.1002/hyp.11277>
- Kuroiwa, D. (1967). Micromeritical properties of snow. *Physics of Snow and Ice, Hokkaido University*, 1(2), 751–772.
- Landry, C. C., Buck, K. A., Raleigh, M. S., & Clark, M. P. (2014). Mountain system monitoring at Senator Beck Basin, San Juan Mountains, Colorado: A new integrative data source to develop and evaluate models of snow and hydrologic processes. *Water Resources Research*, 50(2), 1773–1788. <https://doi.org/10.1002/2013WR013711>
- Lapo, K., Nijssen, B., & Lundquist, J. D. (2019). Evaluation of turbulence stability schemes of land models for stable conditions. *Journal of Geophysical Research-Atmospheres*, 124(6), 3072–3089. <https://doi.org/10.1029/2018JD028970>
- Lawrence, D. M., Fisher, R. A., Koven, C. D., Oleson, K. W., Swenson, S. C., Bonan, G., Collier, N., Ghimire, B., Kampenhout, L., Kennedy, D., Kluzek, E., Lawrence, P. J., Li, F., Li, H., Lombardozzi, D., Riley, W. J., Sacks, W. J., Shi, M., Vertenstein, M., ... Zeng, X. (2019). The community land model version 5: Description of new features, benchmarking, and impact of forcing uncertainty. *Journal of Advances in Modelling Earth Systems*, 11(12), 4245–4287. <https://doi.org/10.1029/2018ms001583>
- LeMone, M. A., Angevine, W. M., Bretherton, C. S., Chen, F., Dudhia, J., Fedorovich, E., Katsaros, K. B., Lenschow, D. H., Mahrt, L., Patton, E. G., Sun, J., Tjernström, M., & Weil, J. (2019). 100 years of Progress in boundary layer meteorology. *Meteorological Monographs*, 59, 9.1–9.85. <https://doi.org/10.1175/amsmonographs-d-18-0013.1>
- Libbrecht, K. G. (2019). Snow crystals. *arXiv preprint arXiv:1910.06389*.
- Liston, G. E., & Elder, K. (2006). A distributed snow-evolution modelling system (SnowModel). *Journal of Hydrometeorology*, 7(6), 1259–1276.
- Lundberg, A., & Halldin, S. (2001). Snow interception evaporation. Review of measurement techniques, processes, and models. *Theoretical and Applied Climatology*, 70(1–4), 117–133.
- Lundberg, A., Nakai, Y., Thunehed, H., & Halldin, S. (2004). Snow accumulation in forests from ground and remote-sensing data. *Hydrological Processes*, 18(10), 1941–1955. <https://doi.org/10.1002/hyp.1459>
- Lundquist, J. D., Dickerson-Lange, S. E., Lutz, J. A., & Cristea, N. C. (2013). Lower forest density enhances snow retention in regions with warmer winters: A global framework developed from plot-scale observations and modelling. *Water Resources Research*, 49(10), 6356–6370.
- Lundquist, J. D., Neiman, P. J., Martner, B., White, A. B., Gottas, D. J., & Ralph, F. M. (2008). Rain versus snow in the Sierra Nevada, California: Comparing Doppler profiling radar and surface observations of melting level. *Journal of Hydrometeorology*, 9(2), 194–211. <https://doi.org/10.1175/2007jhm853.1>
- Mahat, V., & Tarboton, D. G. (2014). Representation of canopy snow interception, unloading and melt in a parsimonious snowmelt model. *Hydrological Processes*, 28(26), 6320–6336. <https://doi.org/10.1002/hyp.10116>
- Martin, K. A., Van Stan, J. T., II, Dickerson-Lange, S. E., Lutz, J. A., Berman, J. W., Gersonde, R., & Lundquist, J. D. (2013). Development and testing of a snow interceptometer to quantify canopy water storage and interception processes in the rain/snow transition zone of the North Cascades, Washington, USA. *Water Resources Research*, 49(6), 3243–3256. <https://doi.org/10.1002/wrcr.20271>
- Mazzotti, G., Currier, W. R., Deems, J. S., Pflug, J. M., Lundquist, J. D., & Jonas, T. (2019). Revisiting snow cover variability and canopy structure within forest stands: Insights from airborne lidar data. *Water Resources Research*, 55(7), 6198–6216. <https://doi.org/10.1029/2019WR024898>
- Mazzotti, G., Essery, R., Moeser, C. D., & Jonas, T. (2020). Resolving small-scale forest snow patterns using an energy balance snow model with a one-layer canopy. *Water Resources Research*, 56(1), e2019WR026129. <https://doi.org/10.1029/2019WR026129>
- Mazzotti, G., Essery, R., Webster, C., Malle, J., & Jonas, T. (2020). Process-level evaluation of a hyper-resolution forest snow model using distributed multisensor observations. *Water Resources Research*, 56(9), e2020WR027572. <https://doi.org/10.1029/2020WR027572>
- Merriam, R. A. (1960). A note on the interception loss equation. *Journal of Geophysical Research*, 65(11), 3850–3851.
- Miller, D. H. (1962). Snow in the trees: Where does it go? *Proceedings of the Western Snow Conference*, 30, 21–27.
- Miller, D. H. (1966). *Transport of intercepted snow from trees during snow storms*. Pacific Southwest Forest and Range Experiment Station, Forest Service.
- Moeser, D., Mazzotti, G., Helbig, N., & Jonas, T. (2016). Representing spatial variability of forest snow: Implementation of a new interception model. *Water Resources Research*, 52(2), 1208–1226. <https://doi.org/10.1002/2015wr017961>
- Moeser, D., Stähli, M., & Jonas, T. (2015). Improved snow interception modelling using canopy parameters derived from airborne LiDAR data. *Water Resources Research*, 51(7), 5041–5059. <https://doi.org/10.1002/2014wr016724>
- Murray, F. W. (1966). On the computation of saturation vapour pressure.
- Nakaya, U. (1954). *Formation of snow crystals*. (Vol. 3), Snow, Ice and Permafrost Research Establishment, Corps of Engineers, US Army. <http://hdl.handle.net/11681/2727>.
- Niu, G.-Y., & Yang, Z. L. (2004). Effects of vegetation canopy processes on snow surface energy and mass balances. *Journal of Geophysical Research-Atmospheres*, 109, D23111. <https://doi.org/10.1029/2004JD004884>
- Niu, G.-Y., Yang, Z.-L., Mitchell, K. E., Chen, F., Ek, M. B., Barlage, M., Kumar, A., Manning, K., Niyogi, D., Rosero, E., Tewari, M., & Xia, Y. (2011). The community Noah land surface model with multiparameterization options (Noah-MP): 1. Model description and evaluation with local-scale measurements. *Journal of Geophysical Research-Atmospheres*, 116, D12109. <https://doi.org/10.1029/2010jd015139>
- Perket, J. (2015). *Diagnosis and Improvement of Cryosphere Shortwave Radiation Biases in Global Climate Models* (PhD thesis). University of Michigan. Retrieved from <http://hdl.handle.net/2027.42/113453>
- Pfister, R., & Schneebeli, M. (1999). Snow accumulation on boards of different sizes and shapes. *Hydrological Processes*, 13(14–15), 2345–2355.
- Pflug, J. M., Liston, G. E., Nijssen, B., & Lundquist, J. D. (2019). Testing model representations of snowpack liquid water percolation across multiple climates. *Water Resources Research*, 55(6), 4820–4838. <https://doi.org/10.1029/2018WR024632>
- Pomeroy, J., & Schmidt, R. (1993). *The use of fractal geometry in modelling intercepted snow accumulation and sublimation*. Paper presented at the Proceedings of the Eastern Snow Conference.
- Pomeroy, J. W., Gray, D. M., Brown, T., Hedstrom, N. R., Quinton, W. L., Granger, R. J., & Carey, S. K. (2007). The cold regions hydrological model: a platform for basing process representation and model structure on physical evidence. *Hydrological Processes*, 21, 2650–2667. <https://doi.org/10.1002/hyp.6787>
- Qu, X., & Hall, A. (2014). On the persistent spread in snow-albedo feedback. *Climate Dynamics*, 42(1), 69–81. <https://doi.org/10.1007/s00382-013-1774-0>
- Raleigh, M. S., & Lundquist, J. D. (2012). Comparing and combining SWE estimates from the SNOW-17 model using PRISM and SWE reconstruction. *Water Resources Research*, 48, W01506. <https://doi.org/10.1029/2011wr010542>
- Reuelto, J., López-Moreno, J. I., Azorin-Molina, C., & Vicente-Serrano, S. M. (2015). Canopy influence on snow depth distribution in a pine stand determined from terrestrial laser data. *Water Resources Research*, 51(5), 3476–3489. <https://doi.org/10.1002/2014WR016496>
- Rittger, K., Raleigh, M. S., Dozier, J., Hill, A. F., Lutz, J. A., & Painter, T. H. (2020). Canopy adjustment and improved cloud detection for remotely sensed snow cover mapping. *Water Resources Research*, 56(6), e2019WR024914. <https://doi.org/10.1029/2019WR024914>

- Roesch, A., Wild, M., Gilgen, H., & Ohmura, A. (2001). A new snow cover fraction parametrization for the ECHAM4 GCM. *Climate Dynamics*, 17(12), 933–946.
- Roth, T. R., & Nolin, A. W. (2019). Characterizing maritime snow canopy interception in Forested Mountains. *Water Resources Research*, 55, 4564–4581. <https://doi.org/10.1029/2018wr024089>
- Rutter, N., Essery, R., Pomeroy, J., Altimir, N., Andreadis, K., Baker, I., Barr, A., Bartlett, P., Boone, A., Deng, H., Douville, H., Dutra, E., Elder, K., Ellis, C., Feng, X., Gelfan, A., Goodbody, A., Gusev, Y., Gustafsson, D., ... Yamazaki, T. (2009). Evaluation of forest snow processes models (SnowMIP2). *Journal of Geophysical Research*, 114, D06111. <http://dx.doi.org/10.1029/2008jd011063>.
- Satterlund, D. R., & Haupt, H. F. (1967). Snow catch by Conifer crowns. *Water Resources Research*, 3(4), 1035–1039. <https://doi.org/10.1029/WR003i004p01035>
- Satterlund, D. R., & Haupt, H. F. (1970). The disposition of snow caught by conifer crowns. *Water Resources Research*, 6(2), 649–652. <https://doi.org/10.1029/WR006i002p00649>
- Sazaki, G., Zepeda, S., Nakatsubo, S., Yokomine, M., & Furukawa, Y. (2012). Quasi-liquid layers on ice crystal surfaces are made up of two different phases. *Proceedings of the National Academy of Sciences*, 109(4), 1052–1055. <https://doi.org/10.1073/pnas.1116685109>
- Schmidt, R. A. (1972). *Sublimation of wind-transported snow: a model* (Vol. 90). Rocky Mountain Forest and Range Experiment Station, Forest Service, US.
- Schmidt, R. A. (1991). Sublimation of snow intercepted by an artificial conifer. *Agricultural and Forest Meteorology*, 54(1), 1–27.
- Schmidt, R. A., & Gluns, D. R. (1991). Snowfall interception on branches of three conifer species. *Canadian Journal of Forest Research*, 21(8), 1262–1269.
- Sexstone, G. A., Clow, D. W., Fassnacht, S. R., Liston, G. E., Hiemstra, C. A., Knowles, J. F., & Penn, C. A. (2018). Snow sublimation in mountain environments and its sensitivity to forest disturbance and climate warming. *Water Resources Research*, 54(2), 1191–1211. <https://doi.org/10.1002/2017WR021172>
- Shampine, L. F., & Reichelt, M. W. (1997). The Matlab ODE suite. *SIAM Journal on Scientific Computing*, 18(1), 1–22.
- Shidei, T. (1952). Study of the fallen snow on the forest trees. I. *Bulletin of the Government Forest Experiment Station*, 54, 115–164.
- Stewart, R. E., Thériault, J. M., & Henson, W. (2015). On the characteristics of and processes producing winter precipitation types near 0°C. *Bulletin of the American Meteorological Society*, 96(4), 623–639. <https://doi.org/10.1175/bams-d-14-00032.1>
- Storck, P. (2000). Trees, snow and flooding: An investigation of forest canopy effects on snow accumulation and melt at the plot and watershed scales in the Pacific northwest.
- Storck, P., Lettenmaier, D. P., & Bolton, S. M. (2002). Measurement of snow interception and canopy effects on snow accumulation and melt in a mountainous maritime climate, Oregon, United States. *Water Resources Research*, 38(11), 5-1–5-16.
- Strasser, U., Bernhardt, M., Weber, M., Liston, G. E., & Mauser, W. (2007). Is snow sublimation important in the alpine water balance? *The Cryosphere Discussions*, 1(2), 303–350.
- Strasser, U., Warscher, M., & Liston, G. E. (2011). Modelling snow-canopy processes on an idealized mountain. *Journal of Hydrometeorology*, 12(4), 663–677. <https://doi.org/10.1175/2011jhm1344.1>
- Sun, N., Wigmosta, M., Zhou, T., Lundquist, J., Dickerson-Lange, S., & Cristea, N. (2018). Evaluating the functionality and streamflow impacts of explicitly modelling forest-snow interactions and canopy gaps in a distributed hydrologic model. *Hydrological Processes*, 32(13), 2128–2140. <https://doi.org/10.1002/hyp.13150>
- Teich, M., Giunta, A. D., Hagenmuller, P., Bebi, P., Schneebeli, M., & Jenkins, M. J. (2019). Effects of bark beetle attacks on forest snowpack and avalanche formation – Implications for protection forest management. *Forest Ecology and Management*, 438, 186–203. <https://doi.org/10.1016/j.foreco.2019.01.052>
- Thackeray, C. W., & Fletcher, C. G. (2016). Snow albedo feedback: Current knowledge, importance, outstanding issues and future directions. *Progress in Physical Geography: Earth and Environment*, 40(3), 392–408. <https://doi.org/10.1177/0309133315620999>
- Thackeray, C. W., Fletcher, C. G., & Derksen, C. (2014). The influence of canopy snow parameterizations on snow albedo feedback in boreal forest regions. *Journal of Geophysical Research-Atmospheres*, 119(16), 9810–9821.
- Thorpe, A., & Mason, B. (1966). The evaporation of ice spheres and ice crystals. *British Journal of Applied Physics*, 17(4), 541–548.
- USACE. (1956). *Snow Hydrology: Summary Rep. of the Snow Investigations*. North Pacific Division.
- Vuyovich, C. M., Jacobs, J. M., & Daly, S. F. (2014). Comparison of passive microwave and modelled estimates of total watershed SWE in the continental United States. *Water Resources Research*, 50(11), 9088–9102. <https://doi.org/10.1002/2013WR014734>
- Watanabe, S., & Ozeki, J. (1964). Study of fallen snow on forest trees (II). Experiment on the snow crown of the Japanese cedar. *Jap. Govt. Forest Exp. Sta. Bull*, 169, 121–140.
- Wayand, N. E., Clark, M. P., & Lundquist, J. D. (2017). Diagnosing snow accumulation errors in a rain-snow transitional environment with snow board observations. *Hydrological Processes*, 31(2), 349–363. <https://doi.org/10.1002/hyp.11002>
- Wayand, N. E., Stimberis, J., Zagrodnik, J. P., Mass, C. F., & Lundquist, J. D. (2016). Improving simulations of precipitation phase and snowpack at a site subject to cold air intrusions: Snoqualmie pass, WA. *Journal of Geophysical Research-Atmospheres*, 121(17), 9929–9942.
- Webster, C., & Jonas, T. (2018). Influence of canopy shading and snow coverage on effective albedo in a snow-dominated evergreen needleleaf forest. *Remote Sensing of Environment*, 214, 48–58. <https://doi.org/10.1016/j.rse.2018.05.023>
- White, J. C., Coops, N. C., Wulder, M. A., Vastaranta, M., Hilker, T., & Tompalski, P. (2016). Remote sensing technologies for enhancing forest inventories: A review. *Canadian Journal of Remote Sensing*, 42(5), 619–641. <https://doi.org/10.1080/07038992.2016.1207484>

How to cite this article: Lundquist, J. D., Dickerson-Lange, S., Gutmann, E., Jonas, T., Lumbrazo, C., & Reynolds, D. (2021). Snow interception modelling: Isolated observations have led to many land surface models lacking appropriate temperature sensitivities. *Hydrological Processes*, 35(7), e14274. <https://doi.org/10.1002/hyp.14274>